Fungal melanin suppresses airway epithelial chemokine secretion through blockade of calcium fluxing

Jennifer L. Reedy[1,2,#], Kirstine Nolling Jensen[1,2,#], Arianne J. Crossen[1], Kyle J. Basham[1], Rebecca A. Ward[1], Christopher M. Reardon[1], Hannah Brown Harding[1,2], Olivia W. Hepworth[1,2], Patricia Simaku[1], Geneva N. Kwaku[1], Kazuya Tone[3,4], Janet A. Willment[3,5], Delyth M. Reid[3], Mark H.T. Stappers[3,5], Gordon D. Brown[3,5], Jayaraj Rajagopal[6,7,8,9], Jatin M. Vyas[1,2,*]

[1] Department of Medicine, Division of Infectious Diseases, Massachusetts General Hospital, Boston, MA, 02114, USA

[2] Harvard Medical School, Boston, MA, 02115, USA

[3] Aberdeen Fungal Group, University of Aberdeen, Institute of Medical Sciences, Foresterhill, Aberdeen, United Kingdom

[4] Division of Respiratory Diseases, Department of Internal Medicine, The Jikei University School of Medicine, Tokyo, Japan

[5] MRC Centre for Medical Mycology, University of Exeter, Exeter, United Kingdom

[6] Center for Regenerative Medicine, Massachusetts General Hospital, Boston, MA, 02114, USA

[7] Division of Pulmonary and Critical Care Medicine, Department of Medicine, Massachusetts General Hospital, Boston, MA, 02114, USA

[8] Harvard Stem Cell Institute, Cambridge, MA, 02138, USA

23 [9] Klarman Cell Observatory, Broad Institute of Massachusetts Institute of Technology
24 and Harvard, Cambridge, MA, 02142, USA
25 *Correspondence: jvyas@mgh.harvard.edu
26 [#]Co-first authors
27

28 ## Summary

29 Respiratory infections caused by the human fungal pathogen *Aspergillus fumigatus* are a major
30 cause of mortality for immunocompromised patients. Exposure to these pathogens occurs
31 through inhalation, although the role of the respiratory epithelium in disease pathogenesis has
32 not been fully defined. Employing a primary human airway epithelial model, we demonstrate that
33 fungal melanins potently block the post-translational secretion of the chemokines CXCL1 and
34 CXCL8 independent of transcription or the requirement of melanin to be phagocytosed, leading
35 to a significant reduction in neutrophil recruitment to the apical airway both *in vitro* and *in vivo*.
36 *Aspergillus*-derived melanin, a major constituent of the fungal cell wall, dampened airway
37 epithelial chemokine secretion in response to fungi, bacteria, and exogenous cytokines.
38 Furthermore, melanin muted pathogen-mediated calcium fluxing and hindered actin filamentation.
39 Taken together, our results reveal a critical role for melanin interaction with airway epithelium in
40 shaping the host response to fungal and bacterial pathogens.
41

42 **Keywords:** airway epithelium, *Aspergillus*, melanin, innate immunity, host-pathogen interaction,
43 fungal immunology

Introduction

Aspergillus fumigatus is the most prominent respiratory fungal pathogen and causes a spectrum of clinical manifestations ranging from allergic disease to severe invasive infections. Despite the ubiquity of this fungal pathogen in the environment, only ~10% of immunocompromised patients (*e.g.,* neutropenic or allogenic bone marrow transplant recipients) develop invasive aspergillosis (IA), indicating that other factors play a significant role in determining the true risk for this infection[1]. In addition to infection associated with the immunocompromised state, there is an increased risk of IA following pulmonary viral infections (*e.g.,* influenza, SARS-CoV-2) and in those with underlying lung disease (*e.g.,* asthma, cystic fibrosis [CF], chronic obstructive pulmonary disease [COPD])[2-5]. The mortality from *Aspergillus*-related pulmonary disease remains unacceptably high (>50%), coinciding with elevated rates of *Aspergillus* multidrug resistance[6-8]. Despite this, the mechanistic interactions governing the invasion of *Aspergillus* at its first point of contact with the host, the airway epithelium, remains poorly understood.

In immune cells, activation of pattern recognition receptors (PRRs), such as the C-type lectin receptor (CLRs), Toll-like receptors (TLRs), NOD-like receptors (NLRs), and Rig-I-like receptors, mediate fungal recognition of cell wall components and subsequent host responses[9]. The cell wall of *Aspergillus* is primarily composed of polysaccharides, including galactosaminogalactan, galactomannan, β-1,3 glucan, β-1,4 glucan, and chitin[10]. Most humans are exposed to *Aspergillus* through the inhalation of conidia, the reproductive propagules of the fungus, which range from 2-3 μm in size and are easily aerosolized in the environment[11,12]. In addition to the typical cell wall components, *Aspergillus* conidia are surrounded by a hydrophobic rodlet and 1,8-dihydroxy naphthalene (DHN) melanin layers[10,12]. Once inhaled by the host, conidia swell and shed these outer layers, exposing the carbohydrate matrix of the cell wall. In immune cells, fungal melanin possesses the remarkable capacity to absorb reactive oxygen species (ROS) and blunt pro-inflammatory cascades, serving as a key virulence factor for many

69 pathogens, including *Aspergillus*[13-19]. Amelanotic strains of clinically relevant fungal pathogens
70 lose their capacity to mount successful infections in mammalian host model systems, indicating
71 that melanin plays a key and non-redundant role in virulence. Indeed, the presence of melanized
72 *Aspergillus* leads to blockage of phagosome biogenesis[20] and removal of the melanin in the
73 phagosome is required to reprogram macrophage metabolism, promoting an antifungal
74 response[21].

75 Clinical data and current literature indicate that several immune system components are
76 critical for the recognition and swift clearance of fungal pathogens. Still, the rules governing the
77 inflammatory responses to fungi in the lungs are poorly understood. Past studies have focused
78 on innate and adaptive immune cells but have often overlooked a key player in respiratory
79 infections: the airway epithelium - the primary point of contact for inhaled conidia[22-25]. The
80 conducting airways are sites of *Aspergillus* colonization and invasion[22-25]. Fortunately, *in vitro*
81 differentiation of primary airway basal cells recapitulates the true diversity of conducting airway
82 epithelium with all of the relevant common (basal, ciliated, club, goblet) and rare (ionocytes, tuft,
83 neuroendocrine) cell types in pseudostratified layers, enabling mechanistic studies *ex vivo*[26].
84 Additionally, these cells form polarized barriers and enable the investigation of basolateral and
85 apical epithelial responses when grown at air-liquid interface (ALI)[27,28]. While the primary human
86 airway epithelial cell (hAEC) ALI model may not fully recapitulate the *in vivo* environment (*e.g.,*
87 lacks resident immune cells, endothelial cells, fibroblasts), this model offers the advantages of a
88 highly pliable system to conduct mechanistic studies without compromising relevant human
89 physiology[28-30] and allow us to pinpoint mechanisms specific to the interaction of the epithelium
90 and inhaled conidia where the microbe first encounters host defense. In addition to utilizing this
91 system, we also use the airway epithelial cell line H292, a mucoepitheliod non-small cell lung
92 carcinoma cell line, which has previously been used extensively in modeling airway epithelial
93 responses to bacterial pathogens. While this cell line does not capture the cellular diversity of the
94 airway epithelium, it is well-suited to mechanistic studies due to cellular uniformity. We previously

95 demonstrated a role for melanin in immune response to *Aspergillus fumigatus* orchestrated by
96 airway epithelium using both primary hAEC and H292 epithelial models[28]. We observed that
97 airway epithelium infected with *A. fumigatus* lacking DHN melanin promoted greater
98 transepithelial migration of neutrophils than wildtype conidia. The mechanism by which melanin
99 modulates epithelial-mediated neutrophil transmigration remains unknown.

100 In the present study, we leveraged primary hAEC to demonstrate that purified fungal
101 melanin at the apical surface of epithelial cells blocked migration of neutrophils and blunted the
102 apical secretion of chemoattractant chemokines. We determined that DHN melanin suppression
103 of neutrophil transmigration and chemokines occured in response to both fungal and bacterial
104 pathogens. Furthermore, L-DOPA melanin from *Cryptococcus neoformans* and other
105 commercially available synthetic melanins inhibited CXCL8 (also known as IL-8) secretion,
106 showing these effects were not unique to DHN melanin, but rather is a preserved property of
107 fungal melanins. We determined that fungal melanin abolished the apical-basolateral CXCL8
108 gradient as a mechanism to block neutrophil recruitment. We demonstrated that melanin
109 suppressed secretion, but not translation or transcription, of CXCL8 in airway epithelium in a
110 phagocytosis-independent manner. Lastly, we unveiled melanin exerts effects through dampened
111 calcium fluxing and disrupted actin filamentation in airway epithelium. Together, these data
112 indicated that fungal melanin inhibits epithelial-mediated inflammation through blocking calcium
113 signaling and the secretion of critical pro-inflammatory chemokines.

114

115 # Results

116 ### *Aspergillus melanin inhibits transepithelial migration of primary neutrophils*

117 We previously demonstrated that hAEC induce neutrophil transmigration upon stimulation with *A.*
118 *fumigatus* wildtype conidia[28]. However, induction of neutrophil transmigration required at least 4h
119 of infection with *A. fumigatus* in contrast to the bacterial pathogen, *Pseudomonas aeruginosa*,

120 which induced robust neutrophil transmigration within 1h[28]. Furthermore, *Aspergillus* conidia that
121 lacked the ability to produce DHN melanin (*ΔpksP*) induced neutrophil transmigration within 1h of
122 infection similarly to *P. aeruginosa*, suggesting that melanin was blocking hAEC responses to
123 resting conidia[28]. Although prior studies identified MelLec as a receptor for DHN melanin in
124 endothelial cells and myeloid cells[31-33], primary hAECs and H292 cell line lacked this receptor
125 (**Supplementary Figure 1**), suggesting that the effects of fungal melanin is exerted through
126 alternative mechanisms. Thus, we hypothesized that melanin could act via two mechanisms to
127 block neutrophil migration: melanin could actively downregulate pro-inflammatory responses or
128 serve as a passive barrier to prevent host access to immunostimulatory epitopes on the fungal
129 cell wall. To test these hypotheses, we performed mixing studies with *A. fumigatus* melanin ghosts
130 and amelanotic *ΔpksP* conidia. Generation of melanin ghosts is a well-described technique in
131 which melanized conidia are biochemically and enzymatically degraded to strip all cellular
132 components except a rigid shell of purified melanin resembling the original size and shape of the
133 conidia[20,34-38]. To ascertain whether melanin coating of conidia was required for its inhibitory
134 function, we stimulated primary hAEC with *ΔpksP* conidia alone or in combination with melanin
135 ghosts at the apical side at a ratio of 5:1 melanin ghosts to *ΔpksP* conidia and then measured
136 neutrophil recruitment across the epithelium (basolateral→apical) (**Figure 1a**). Stimulation of
137 hAEC with *ΔpksP* conidia mixed with melanin ghosts dampened neutrophil transmigration when
138 compared to *ΔpksP* alone (**Figure 1b**). As expected, melanin ghosts alone did not stimulate
139 neutrophil transmigration.

140 We next examined if this response seen in primary hAEC extended to the human lung
141 epithelial cell line, H292, which is routinely used to dissect airway responsiveness to bacterial
142 pathogens[39-41]. While these cells do not recapitulate the cellular diversity of the primary airway
143 epithelium, they are well suited to mechanistic studies given their homogeneity, thus we wished
144 to determine if our phenotype could translate to this model system. We observed that infection

145 with *ΔpksP* conidia alone induced more neutrophil recruitment across H292 monolayers
146 compared with *ΔpksP* conidia in the presence of melanin ghosts (**Figure 1c**) recapitulating the
147 primary hAECs findings. Since the melanin in these experiments was applied as discrete particles
148 unable to coat the surface of the *ΔpksP* conidia, these results indicate a model where melanin
149 actively downregulates inflammatory responses rather than acting as a passive barrier on the
150 surface of the conidia.
151

152 **Aspergillus *melanin inhibits secretion of airway epithelial-derived CXCL8 and***
153 ***CXCL1***

154 To understand the mechanism of how neutrophil transmigration was silenced, we performed a
155 Luminex assay using primary human airway epithelium derived from three healthy human donors.
156 Primary hAEC was differentiated at ALI for 16 days prior to stimulation with either media alone
157 (HBSS), *P. aeruginosa* (positive control), three wildtype strains of *A. fumigatus* (CEA10, Af293,
158 B5233), or the amelanotic *A. fumigatus ΔpksP* strain (derived from B5233). CXCL8 and CXCL1
159 (also known as GROα) are two neutrophil chemoattractants produced by the airway epithelium
160 and were the most abundant chemokines specifically induced on the apical side by the mutant
161 *ΔpksP A. fumigatus* strain, but not by wildtype strains (**Figure 2a-b, Supplementary Figure 2**).
162 We confirmed these differences in cytokine expression in H292 cells using both the *ΔpksP* and
163 *ΔpksP* complemented strains (**Figure 2c-d**) to validate the use of these cells for mechanistic
164 studies.

165 To determine if melanin acted through a blockade of epithelial chemokine secretion, we
166 performed mixing studies in which we stimulated with a fixed concentration of *ΔpksP* conidia
167 combined with graded amounts of melanin ghosts. The mixing assay revealed that the addition
168 of melanin ghosts suppressed both CXCL8 and CXCL1 chemokine apical secretion in a dose-
169 dependent manner (**Figure 2e-f**). Melanin ghosts alone applied at the highest concentration did

170 not induce chemokine secretion. To confirm that these results were not due to absorption by
171 melanin ghosts of secreted CXCL8, we examined neutrophil migration to the apical compartment
172 in epithelium exposed to melanin ghosts in the presence and absence of exogenous CXCL8.
173 Indeed, despite the presence of melanin ghosts, exposure to CXCL8 triggered robust neutrophil
174 migration (**Figure 2g**). These data suggest that melanin ghosts block the secretion of CXCL8 and
175 CXCL1 rather than adsorb extracellular chemokines.
176

177 ***The inhibitory effects of Aspergillus melanin extend to other pro-inflammatory***
178 ***stimuli***

179 Thus far, our experiments suggested that melanin was not acting as a passive protective shield,
180 but directly downregulated pro-inflammatory responses. We next sought to determine if fungal
181 melanin anti-inflammatory actions were specific to fungal pathogens or if they represented a more
182 general host-microbe interaction. *P. aeruginosa* is an important bacterial respiratory pathogen
183 frequently found in co-infections with *A. fumigatus* in patients with CF. Therefore, we examined
184 whether *Aspergillus* melanin ghosts could dampen *P. aeruginosa*-induced airway epithelial
185 inflammation. We infected H292 monolayers with *P. aeruginosa* alone or in combination with
186 melanin ghosts for 6h then quantified chemokine secretion. The addition of melanin ghosts
187 suppressed CXCL8 (**Figure 3a**) and CXCL1 (**Supplementary Figure 3a**) release in response to
188 *P. aeruginosa* in a dose-dependent manner. To ensure that the melanin ghosts were not
189 interfering with the ability of *P. aeruginosa* to bind to the epithelium, we confirmed that *P.*
190 *aeruginosa* binding or internalization by the epithelial cells was not altered in the presence of
191 melanin ghosts (**Supplementary Figure 3b**), suggesting that the difference in chemokine
192 secretion was not due to difference in the ability of *P. aeruginosa* to access the cells. Additionally,
193 we performed an LDH cell viability assay that demonstrated no difference in cell viability in the
194 presence of *Pseudomonas* with or without melanin (**Supplementary Figure 3c**).

195 TNFα is a known inducer of secretion of CXCL8 by airway epithelial cells, therefore we
196 hypothesized that melanin ghosts also block cytokine-induced CXCL8 in airway epithelial cells.
197 We stimulated H292 epithelium with recombinant human TNFα for 6h in the presence of absence
198 of melanin ghosts then quantified CXCL8 secretion in supernatants. The combination of melanin
199 ghosts and TNFα stimulation of epithelial cells failed to secrete CXCL8 compared to stimulation
200 with TNFα alone (**Figure 3b**).
201

202 ***Melanin blocks* Pseudomonas*-induced transepithelial migration of neutrophils***

203 Since co-stimulation of airway epithelium with *P. aeruginosa* and melanin ghosts resulted
204 in a potent decrease of CXCL8 secretion, we examined the role of melanin ghosts in airway
205 epithelial-induced neutrophils transmigration in response to *P. aeruginosa*. While CXCL8 is a
206 known neutrophil chemoattractant that plays a role in epithelial-induced neutrophil
207 transmigration[42,43], recruitment of neutrophils across the epithelium has been linked to other
208 secreted compounds, such as hepoxilin A3, in response to *P. aeruginosa* [44-47]. We stimulated both
209 primary hAEC and H292 with *P. aeruginosa* alone or in combination with melanin ghosts and
210 quantified neutrophil transmigration using a myeloperoxidase assay. The addition of melanin
211 ghosts decreased *P. aeruginosa*-induced neutrophil transmigration (**Figure 3c**), demonstrating
212 that melanin blocked all mediators required for neutrophil recruitment to *Pseudomonas*.
213 To determine if blunting of neutrophil influx occurs in an *in vivo* model of infection, we
214 infected mice with *P. aeruginosa* alone or in combination with melanin ghosts. As predicted, *P.*
215 *aeruginosa* induced potent neutrophil recruitment into the airways of mice; however the number
216 of neutrophils in the bronchoalveolar lavage fluid was significantly decreased in the presence of
217 melanin (**Figure 3d**). Together, these data indicated that modulation of pro-inflammatory
218 processes by melanin ghosts extends to recruitment of neutrophils to the site of infection *in vivo*.
219

220 ***Structurally distinct melanins from diverse fungal sources block airway epithelial***
221 ***CXCL8 expression***

222 Melanins are darkly pigmented molecules created through the polymerization of phenol or indole
223 precursors forming polymers of high molecular weight[48,49]. Despite the ubiquity of melanin
224 pigments across kingdoms (*e.g.,* animals, fungi, insects, helminths), the structure of melanin
225 remains poorly defined. *Aspergillus* and dematiaceous molds produces DHN melanin catalyzed
226 by the polyketide synthase pathway[14-16,50]. However, some fungal pathogens contain melanin
227 derived from L-tyrosine or L-dihydroxyphenylalanine (L-DOPA) produced through the action of
228 tyrosinase or laccase, respectively[34,35,51-56]. One example of laccase-derived melanin occurs in *C.*
229 *neoformans*, an environmental yeast that causes human infections including pneumonia and
230 meningitis. L-DOPA-based melanins are structurally distinct from *Aspergillus* DHN melanin. This
231 structural difference impacts host responses as demonstrated by the recognition of DHN, but not
232 L-DOPA, melanin by the CLR, MelLec or Clec1A, identified on endothelial and immune cells[31-33].
233 To determine if the ability to inhibit the appearance of epithelial-derived CXCL8 in the supernatant
234 was specific to *Aspergillus* DHN melanin, we utilized both *C. neoformans* melanin ghosts and a
235 synthetic tyrosine-based melanin. As strong inducers of epithelial CXCL8, *Pseudomonas* and
236 amelanotic *ΔpksP A. fumigatus* were used to stimulate H292 epithelium in the presence or
237 absence of *C. neoformans* melanin ghosts. Similar to *Aspergillus* melanin ghosts, *Cryptococcus*
238 melanin ghosts suppressed CXCL8 and CXCL1 in the supernatant (**Figure 4a, Supplementary**
239 **Figure 4**).

240 In addition to our *C. neoformans* melanin ghosts, we also tested epithelial responses to a
241 synthetic source of tyrosine-derived melanin. We previously created fungal-like particles (FLP)
242 using purified fungal carbohydrates which associated with amine-coated polystyrene 3 μM
243 microspheres using either chemical conjugation or adsorption[57,58]. Using this technique, we
244 coated beads to create FLP with synthetic L-DOPA and β-1,3 glucan. β-1,3-glucan is a pro-

245 inflammatory carbohydrate found in most fungal cell walls and was added as an additional control
246 to demonstrate that any effect was due to the melanin and not a result of any coating applied to
247 the microspheres. We stimulated H292 monolayers with *P. aeruginosa* either alone or in
248 combination with unmodified FLP (naked beads), L-DOPA melanin-coated FLP, or β-1,3-glucan-
249 coated FLP. We found that combined treatment with *P. aeruginosa* and L-DOPA-coated FLP led
250 to a reduction in CXCL8 secretion, while no difference in CXCL8 secretion was observed when
251 *P. aeruginosa* was combined with either unmodified FLP or β-1,3-glucan-coated FLP (**Figure 4b**).
252 Taken together, these results demonstrate that the immunomodulatory effect of melanin is not
253 specific to *Aspergillus* melanin, but also occurs in response to *C. neoformans* L-DOPA based
254 melanin and a synthetic tyrosine-based melanin.
255

256 ***Melanin abolishes the transepithelial gradient of CXCL8 required for neutrophil***
257 ***transmigration***

258 Since epithelial cells are polarized, they secrete effector molecules selectively to either the apical
259 or basolateral compartments or bidirectionally. Neutrophil transmigration to the apical surface (*i.e.*
260 airway), requires the creation of a chemokine gradient established by differential secretion at the
261 apical and basolateral surfaces[59-61]. To understand whether apical stimulation with melanin
262 affected only apical chemokine secretion or both the apical and basolateral compartments, we
263 stimulated H292 monolayers grown on Transwells with *P. aeruginosa* in the presence or absence
264 of melanin ghosts and collected supernatants from both the apical and basolateral compartments.
265 H292 were chosen to model this interactions because basolateral chemokine secretion by hAECs,
266 even in the presence of *P. aeruginosa* was below the limit of detection (*data not shown*).
267 Stimulation with *P. aeruginosa* induced higher release of CXCL8 on the apical surface of the
268 epithelium when compared to the basolateral surface (**Figure 5a**). The combination of *P.*
269 *aeruginosa* with *Aspergillus* melanin ghosts significantly decreased both apical and basolateral

270 epithelium CXCL8 secretion when compared with *Pseudomonas* alone. Furthermore, this co-
271 stimulation effectively abolished the apical-basolateral chemokine gradient generated by *P.*
272 *aeruginosa*.
273

274 ***Melanin induces durable impact on CXCL8 secretion***

275 Thus far, our experiments examined the impact of melanin ghosts for short durations (6h or less).
276 Thus, we sought to understand whether melanin stimulation of epithelium produced a lasting
277 effect at the epithelium or was a transient suppression of chemokine release. Melanin ghosts
278 were durable and were not degraded in our cell culture systems as shown in previous studies
279 utilizing melanin ghosts[19,62,63]. We stimulated H292 epithelium with *P. aeruginosa* or TNFα in
280 combination with melanin ghosts for 24h. After 24h stimulation, there was a persistent reduction
281 of apical CXCL8 secretion by epithelial cells co-stimulated melanin ghosts compared with either
282 *P. aeruginosa* or TNFα alone (**Figure 5b**), supporting the hypothesis that melanin silenced the
283 airway epithelium to prevent inflammation, not simply delaying the initiation of response.
284

285 ***Melanin suppression of chemokine secretion is independent of phagocytosis of***
286 ***melanin or* de novo *transcription***

287 To determine the mechanism by which melanin blocked CXCL8 secretion by airway epithelial
288 cells, we first examined whether phagocytosis of melanin ghosts was required. H292 epithelium
289 were pre-treated with cytochalasin D, an inhibitor of actin polymerization that effectively blocks
290 phagocytosis, then stimulated with either TNFα alone or in combination with *Aspergillus* melanin
291 ghosts. Melanin ghosts inhibited TNFα–induced CXCL8 secretion both in the presence and
292 absence of cytochalasin D, suggesting that phagocytosis of melanin ghosts was not required for
293 its anti-inflammatory action (**Figure 6a**). Cytochalasin D alone increased basal levels of secretion
294 compared to media alone as shown previously in H292 cells[64].

295 We next investigated if melanin-induced transcription was required for CXCL8
296 suppression using the transcription inhibitor, actinomycin D. Following pre-treatments with vehicle
297 control or actinomycin D, epithelial cells were incubated with TNFα, TNFα plus *Aspergillus*
298 melanin ghosts, or melanin ghosts alone. TNFα induction of CXCL8 required CXCL8
299 transcription[65], therefore as expected addition of actinomycin D blocked TNFα–induced CXCL8
300 secretion (**Figure 6b**). Airway epithelial cells produce basal levels of CXCL8 as demonstrated by
301 the media only controls where there was low, but detectable concentrations of CXCL8. Melanin
302 ghosts suppressed basal levels of CXCL8 secretion by H292 cells. Actinomycin D-mediated
303 inhibition of transcription did not alter melanin ghosts-induced suppression of basal CXCL8
304 (**Figure 6b**). Together, these data revealed that the suppression of CXCL8 secretion was
305 independent of phagocytosis and *de novo* gene transcription.
306

307 ***Melanin exerts a post-translational blockade on CXCL8 secretion***

308 To understand further how melanin acted at a cellular level, we sought to illuminate the
309 mechanism by which melanin interfered with CXCL8 secretion by epithelial cells. Therefore, we
310 performed paired experiments, in which we stimulated both primary hAEC cultures
311 (**Supplementary Figure 5a-b**) or H292 monolayers (**Figure 6c-d**) with media alone, wildtype *A.*
312 *fumigatus* conidia, *ΔpksP* conidia alone or in combination with melanin ghosts, *P. aeruginosa*
313 alone or in combination with melanin ghosts, and melanin ghosts alone. CXCL8 transcription was
314 induced by all stimuli compared with media treatment alone and no significant difference in
315 transcript levels between our pro-inflammatory stimuli (*ΔpksP* or *P. aeruginosa)* either alone or in
316 combination with melanin, demonstrating that melanin ghosts did not block transcription of CXCL8
317 (**Figure 6c, Supplementary Figure 5a**). Immunoblotting of epithelial cell lysates revealed
318 increased intracellular CXCL8 in cells treated with melanin ghosts in combination with a pro-
319 inflammatory stimulant (*i.e., ΔpksP* conidia or *P. aeruginosa*) compared to cells treated with the

320 pro-inflammatory stimulant alone (**Figure 6d, Supplementary Figure 5b**). Interestingly, we
321 observed an increase of intracellular CXCL8 protein within cells treated with melanin ghosts,
322 which is in direct contrast to the decrease in extracellular release of CXCL8 demonstrated by
323 ELISA. These data demonstrated that the difference in extracellular CXCL8 protein in epithelial
324 supernatants was not due to difference in either transcription or translation of the CXCL8 protein.
325 Taken together our results revealed that melanin interfered with CXCL8 signaling by airway
326 epithelium through a post-translational blockade of chemokine secretion.
327

328 ***Fungal melanin blocked calcium fluxing in epithelial cells***

329 Given our data suggesting melanin exerts its effects through a transcription/translation-
330 independent mechanism, we hypothesized that fungal melanin mediated chemokine reductions
331 through perturbation of an early signaling pathway- calcium fluxing. To examine if fungal melanin
332 modulated host responses through calcium signaling, we measured calcium fluxing over time in
333 airway epithelium stimulated by ionomycin and calcium chloride or media alone in the presence
334 and absence of melanin ghosts by plate assay (**Figure 7a**) and confocal microscopy (**Figure 7b**).
335 As expected, treatment with ionomycin and calcium chloride induced robust calcium fluxing, with
336 a peak around 10 minutes. Melanin potently muted calcium fluxing to similar levels as
337 unstimulated cells (media alone). Together, these data suggest that fungal melanin modulates
338 epithelial host responses through calcium signaling.
339

340 ***Melanin disrupts actin structure in airway epithelial cells***

341 Our results demonstrate chemokine secretion, but not production, is blocked by fungal melanin.
342 To examine whether actin polymerization, which can be mediated by calcium, changes in airway
343 epithelium in the presence of *A. fumigatus* melanin ghosts, we imaged phalloidin-stained epithelial
344 cells pre-treated with *P. aeruginosa* or media alone with or without melanin ghosts. Phalloidin
345 enables visualization of actin filaments (*i.e.,* F actin). In the presence of fungal melanin, epithelial

346 cells showed dampened levels of phalloidin staining (**Figure 8a**). Using the same experimental
347 groups, we next measured the amount of F and G actin by immunoblotting. We added latrunculin
348 A (an inhibitor of actin polymerization), phalloidin (positive F actin control), and DMSO vehicle as
349 additional controls. These results confirmed reduced F actin levels (**Figure 8b**), indicating that the
350 fungal melanin disrupts actin polymerization resulting in diminished chemokine secretion in
351 response to inflammatory stimulus.
352

353 ## Discussion

354 Humans are exposed to most fungal pathogens, including *A. fumigatus*, through inhalation of fungal
355 particles including conidia, yeasts, or hyphal fragments. Upon inhalation, *Aspergillus* conidia are
356 deposited throughout the host airways, however we lack a detailed understanding of the role that
357 respiratory epithelium plays in directing the outcome of host-pathogen interaction towards clearance,
358 invasion, or allergic disease. Here, we utilized primary, well differentiated hAEC at ALI and the
359 monomorphic H292 cell line to demonstrate that fungal melanin actively downregulates airway
360 epithelial-driven chemokine responses. Our results demonstrate that *Aspergillus* melanin potently
361 blocks epithelial-driven chemokines via a post-translational inhibition of secretion by muting calcium
362 fluxing and disruption of actin polymerization, resulting in the ablation of the chemokine gradient that
363 silences neutrophil transmigration.

364 The primary hAEC model is powerful model as it recapitulates the pseudostratified
365 structure and cellular diversity of conducting airway epithelium, enabling study of rare populations
366 and the interplay of epithelial cells in disease[26]. Most epithelial cell types cannot be grown in pure
367 cultures, limiting our understanding of the role of specific epithelial cell subtypes in the
368 pathogenesis of disease. While this system has clear advantages over oncogenic and
369 immortalized cell lines, we also confirmed our phenotype in the the cell line, H292, a
370 mucoepitheliod non-small cell lung carcinoma cell line, as this reagent has previously been used
371 extensively in modeling airway epithelial responses to bacterial pathogens[27,39,40,66-68]. While this

372 cell line does not capture the cellular diversity of the airway epithelium, it is well-suited to
373 mechanistic studies due to uniformity of cellular responses and ability to grow large-scale cultures
374 without a dependence on patient sample quality. Importantly, our results demonstrate that
375 melanin effects both primary hAEC and H292 epithelial similarly, indicating that H292 cells can
376 serve as a relevant model system for mechanistic dissection of melanin sensing and response
377 pathways.

378 Prior studies identified an impact on the innate immune sensing of fungal pathogens by
379 fungal melanin. Melanin reprogramed the metabolome of macrophages and prevented LC3-
380 associated phagocytosis of *Aspergillus* conidia through sequestration of calcium preventing
381 calcineurin activation[21,37,69,70]. Additionally, melanin is a known inhibitor of ROS production by
382 phagocytes[12-17], which is an important mechanism of pathogen killing by macrophages and
383 neutrophils. Since the airways are the first point of contact in invasive aspergillosis, we sought to
384 determine the biological role melanin played in innate immune responses. Here, we depict a
385 critical role for fungal melanin in decreasing airway epithelial pro-inflammatory chemokine
386 secretion via a post-translational mechanism, independent of both phagocytosis or *de novo*
387 transcription. A recent study suggested depletion of extracellular CXCL10 and CCL20
388 chemokines by DHN melanin, but not IL-1α or CXCL8[19]. This study indicates that *Aspergillus*
389 melanin binds to some pro-inflammatory cytokines in the extracellular space. While we
390 demonstrate a reduction in CXCL8 and CXCL1 in our epithelial model, our data suggest that this
391 is not largely in part to adsorption by melanin. The mechanisms responsible for recognition of
392 fungal melanin by epithelial cells remains unknown and warrant further studies. MelLec (also
393 known as Clec1A) is a CLR that recognizes *Aspergillus* DHN melanin, but not L-DOPA melanin
394 of *C. neoformans*[31,69]. Both *A. fumigatus* DHN melanin and *C. neoformans* L-DOPA melanin block
395 airway epithelial-derived inflammation suggesting a universal melanin effect at the epithelial
396 surface. Given the specificity of MelLec for only DHN melanin, and the expression of human
397 MelLec is restricted to endothelial cells and innate cells (**Supplementary Figure 1**)[31], the

398 respiratory epithelial response to melanin is likely independent of MelLec. Our experiments
399 suggest that the phagocytosis of melanin particles is not necessary, since cytochalasin D does
400 not block the ability of melanin ghosts to suppress epithelial CXCL8 secretion, suggesting that
401 melanin is interacting with a cell surface receptor or a soluble factor released by epithelial cells.
402 The observations that multiple forms of melanin retain the capacity to blunt the chemokine
403 secretion by airway epithelial cells suggests that human pathogens exploit this pathway to
404 establish successful infection. Indeed, multiple organisms possess melanin including *A.*
405 *fumigatus, C. neoformans,* and *Bordetella pertussis*[16,34,71]*.* Our understanding of melanin is
406 evolving from a structural scaffold that provides protection from the harsh environment it inhabits
407 to a multi-purpose molecule that disables the immune response at multiple steps. Our finding that
408 *Aspergillus* melanin inhibits *P. aeruginosa*-induced airway epithelial chemokine secretion
409 indicates that *Aspergillus* could play a role in dampening inflammation during co-infections
410 common in CF patients. Colonization by *Aspergillus* could enhance the virulence of *P. aeruginosa*
411 in patients by blocking early innate immune cell recruitment to sites of *P. aeruginosa* infection.

412 Our results indicate the suppression of early signaling cascades induced by fungal
413 melanin, specifically calcium signaling. Calcium contributes through key signaling mechanisms in
414 host immunity, such as TLR/CLR signaling, ROS production, and cytokine induction[72,73]. In innate
415 immune cells, calcium has been linked to CXCL8 secretion in response to thapsigargin. Indeed,
416 intracellular calcium stores in neutrophils are required and depletion of this calcium was not
417 sufficient to trigger CXCL8 secretion[74]. Although this phenomenon has not been expanded to
418 airway epithelial cells, thapsigargin increases CXCL8 in immortalized airway epithelium[75]. Prior
419 studies have linked *Aspergillus* melanin to sequestration of calcium inside the phagosome to block
420 LC3-associated phagocytosis in monocytes[70], yet whether melanin impacted calcium-mediated
421 secretion of cytokines and chemokines was not reported. Our data suggest that sequestration of
422 calcium extends beyond inhibition of phagocytosis to include dampened chemokine secretion.
423 We propose that the melanin blunts calcium fluxing resulting in perturbation of actin

424 polymerization and subsequent impairment in the release of CXCL1 and CXCL8. It is important
425 to note that changes in actin polymerization may not be the sole contributor of calcium-mediated
426 signaling in airway epithelial antifungal defense.

427 While we focused primarily on CXCL8 for this work, fungal melanin also inhibited the
428 secretion of CXCL1 (**Figure 2b, Supplementary Figure 3a, and Supplementary Figure 4**).
429 While CXCL8 and CXCL1 are known neutrophil chemoattractants that plays a role in epithelial-
430 induced neutrophil transmigration other secreted compounds are also required for *P. aeruginosa*
431 dependent neutrophil transmigration including hepoxilin A3[44-47]. Melanin ghosts dampened
432 neutrophil transmigration in response to *P.aeruginosa,* indicating that the effect of fungal melanin
433 may have a broad impact on airway epithelial cell secretion. Both CXCL8 and CXCL1 are secreted
434 through the trans-Golgi network. The intracellular accumulation of CXCL8 protein with little
435 detectable extracellular CXCL8 suggests that melanin may interfere with trans-Golgi secretion of
436 CXCL8. Future studies will interrogate both traditional trans-Golgi secretomal pathways, as well
437 as alternative secretion systems, such as IL-1β which is secreted via a gasdermin dependent
438 mechanism, to determine the extent of the melanin secretional blockade.

439 Fungal melanins act as an anti-inflammatory agent at the respiratory epithelium, blocking
440 post-translational secretion of chemokines to recruit host immune cells. *Aspergillus* melanin is
441 required to establish invasive disease as the *⊿pksP* is avirulent in animal models of infection. The
442 mechanism underpinning the virulence defect of the *⊿pksP* strain has long been attributed to
443 melanin blockade of phagosomal maturation and ROS production by innate immune cells, critical
444 requirements for host response to *Aspergillus*. However, our work highlights an additional role for
445 melanin in the host-pathogen interaction, as an anti-inflammatory that prevents airway epithelial
446 chemokine secretion thereby decreasing early recruitment of neutrophils to sites of infection.
447 While there is a clear benefit to the pathogen in preventing inflammatory cell recruitment to the
448 airways, there is potential benefit to the host in dampening host response to melanin at the airway

epithelium. If melanin fails to silence inflammation in some patients this could lead to chronic inflammatory conditions including chronic pulmonary aspergillosis and allergic diseases such as allergic bronchopulmonary aspergillosis and fungal asthma.

Acknowledgements

We would like to thank Drs. Bryan Hurley and Hongmei Mou for insightful discussions regarding our work. Additionally, we would like to thank Dr. George Chamilos for providing melanin ghosts to test in parallel with those created in our own lab. J.L.R was supported by NIH/NIAID grant 1K08AI14755. J.M.V is supported by R01AI150181, R01AI136529, and R21AI152499. GDB acknowledges funding from the MRC Centre for Medical Mycology at the University of Exeter (MR/N006364/2 and MR/V033417/1) and the Wellcome Trust (102705, 217163).

Author Contributions

Conceptualization – Jennifer Reedy, Kirstine Nolling Jensen, and Jatin Vyas. *Investigation* – Jennifer Reedy, Kirstine Nolling Jensen, Arianne Crossen, Kyle J. Basham, Chris Reardon, Hannah Brown Harding, Olivia W. Hepworth, Patricia Simaku, Geneva N. Kwaku, Kazuya Tone, Janet A. Willment, Delyth M. Reid, Mark H.T. Stappers. *Writing* – Jennifer Reedy, Kirstine Nolling Jensen, Rebecca Ward, Arianne Crossen, Jatin Vyas. *Manuscript review and revision* – Arianne Crossen, Kyle Basham, Hannah Brown Harding, Chris Reardon, Olivia W. Hepworth, Patricia Simaku, Geneva N. Kwaku, Kazuya Tone, Janet A. Willment, Delyth M. Reid, Mark H.T. Stappers, Gordon D. Brown. *Resources* – Jennifer Reedy, Jayaraj Rajagopal, Gordon D. Brown Jatin Vyas.

Competing Interests

The authors declare no competing interests.

Data Availability

The data that support the findings of this study are available from the corresponding author upon reasonable request.

478 ## Figure Legends

479 **Figure 1. *Aspergillus* melanin inhibits transepithelial migration of neutrophils. (a)**
480 Schematic of neutrophil migration assay. Neutrophil migration across primary human airway
481 epithelial cells (hAECs) **(b)** or H292 cells **(c)** measured by apical MPO assay following infection
482 (2h hAECs; 1h H292) with 1 x 10^7/cm^2 wildtype B5233 or *ΔpksP A. fumigatus* conidia in the
483 presence or absence of purified *A. fumigatus* melanin ghosts (MG; 5 x 10^7/cm^2). Negative control
484 of media (HBSS) or MG alone were included. Data represents the number of neutrophils as
485 determined by standard curve. Data are represented as mean ± SEM. N=4-6; One-Way ANOVA
486 with Tukey's multiple comparisons test; **p<0.01, ***p<0.001, ****p<0.0001.

487

488 **Figure 2. *Aspergillus* melanin inhibits secretion of airway epithelial-derived CXCL8 and**
489 **CXCL1.** CXCL8 and CXCL1 in apical cell supernatants measured by Luminex **(a-b)** and ELISA
490 **(c-f)**. **(a-b)** Primary hAECs following 4h stimulation by media alone (HBSS), *P. aeruginosa* PAO1
491 strain (PSA), three different wildtype (WT) *A. fumigatus* strains (1 x 10^7/cm^2) or *ΔpksP A.*
492 *fumigatus* conidia (1 x 10^7/cm^2). N=3. See also Figure S2 **(c-d)** H292 cells were stimulated for 4h
493 with HBSS, two WT *A. fumigatus* strains, *ΔpksP* conidia, or *ΔpksP* complemented strain (1 x
494 10^7/cm^2). N=4. **(e-f)** H292 were stimulated for 4h with HBSS, WT B5233 conidia (1x10^7/cm^2),
495 *ΔpksP* conidia (1x10^7/cm^2), *ΔpksP* conidia mixed with increasing concentrations of *Aspergillus*
496 melanin ghosts (MG; 0.1x = 1x10^6/cm^2; 1x = 1x10^7/cm^2; 10x = 1x10^8/cm^2), or MG alone
497 (1x10^8/cm^2). N=3. **(g)** Neutrophil migration to the apical compartment across H292 epithelium
498 pretreated for 1h with MG (1x10^8/cm^2) in the absence and presence of exogenous CXCL8 (3,000
499 pg/mL). N=3. Data are represented as mean ± SEM. One-Way ANOVA with Tukey's multiple
500 comparisons test; *p<0.05, **p<0.01, ***p<0.001, ****p<0.0001 compared to *ΔpksP* alone (a-f) or
501 MG+CXCL8 (g).

502 **Figure 3. The inhibitory effects of *Aspergillus* melanin extended to other pro-inflammatory**
503 **stimuli. (a)** H292 epithelium infected with media alone (HBSS; negative control), *P. aeruginosa*
504 PAO1 strain (PSA) in the absence and presence of increasing *A. fumigatus* melanin ghosts (MG;
505 0.2x= $2x10^6/cm^2$; 1x= $1x10^7/cm^2$; 5x= $5x10^7/cm^2$) or MG alone for 6h. Apical CXCL8 secretion in
506 the supernatant was measured by ELISA. n=3. See also Figure S3. **(b)** Apical CXCL8 secretion
507 was measured by ELISA following a 6h stimulation of H292 cells with HBSS, PSA ± MG, TNFα
508 (100 ng/mL) ± MG, or *Aspergillus* MG alone ($5x10^7/cm^2$). n=3. **(c)** Neutrophil migration across
509 H292 epithelium in response to PSA alone or in the presence of MG or MG alone ($5x10^7/cm^2$)
510 was measured by apical MPO assay. Data represents the number of neutrophils as determined
511 by the standard curve. n=6. **(d)** 6-12-week-old C57BL/6 mice were infected via oropharyngeal
512 aspiration with PSA ($5.85x10^5$) with or without *Aspergillus* MG ($5.85x10^6$) for 4h. The number of
513 neutrophils in the bronchoalveolar lavage fluid was measured by flow cytometry. n=5-6. Data are
514 represented as mean ± SEM. One-Way ANOVA with Tukey's multiple comparisons test; *$p<0.05$,
515 **$p<0.01$, ***$p<0.001$, compared to stimulation alone (*i.e.,* PSA or TNFα alone).
516
517 **Figure 4. Structurally distinct melanins from diverse fungal sources block airway epithelial**
518 **CXCL8. (a)** H292 cells were stimulated for 6h with wildtype *A. fumigatus* (B5233; $1x10^7/cm^2$),
519 *ΔpksP* conidia ($1x10^7/cm^2$) with or without *C. neoformans* H99 melanin ghosts (*Cn*-MG)
520 ($5x10^7/cm^2$), *P. aeruginosa* PAO1 strain (PSA) with or without *Cn*-MG, or *Cn*-MG alone. CXCL8
521 apical secretion was measured by ELISA. See also Figure S4. **(b)** H292 epithelium was infected
522 with PSA in the absence or presence of synthetic L-DOPA-coated FLP ($5x10^7/cm^2$), β-1,3-glucan-
523 coated FLP (BG; $5x10^7/cm^2$), or naked FLP ($5x10^7/cm^2$) for 6h, then apical CXCL8 secretion was
524 measured by ELISA. Media or coated beads alone were included as negative controls. Data are
525 represented as mean ± SEM. n=3; One-Way ANOVA with Dunnett's multiple comparisons test;
526 *$p<0.05$, **$p<0.01$, ****$p<0.0001$ compared to stimulation alone (*i.e., ΔpksP* or PSA alone).

527 **Figure 5. Melanin abolished the transepithelial gradient of CXCL8 required for neutrophil**
528 **transmigration, with a durable impact on CXCL8 secretion. (a)** CXCL8 expression in the
529 media from the apical (A) and basolateral (BL) sides of H292 cells was measured by ELISA. H292
530 cells were infected for 6h with *P. aeruginosa* PAO1 strain (PSA) and *Aspergillus* melanin ghosts
531 (MG; $5x10^7/cm^2$) together or alone. Media alone (HBSS) was used as a negative control. n=6; ~~one~~
532 two-way ANOVA with Sidak's multiple comparisons test. ****p<0.0001. **(b)** An ELISA assessed
533 apical CXCL8 levels following a 24h stimulation with PSA or TNFα (100 ng/mL) in the absence or
534 presence of MG ($5x10^7/cm^2$). n=3; one-way ANOVA with Tukey's multiple comparison test. Data
535 are represented as mean ± SEM. ***p<0.001, ****p<0.0001.
536
537 **Figure 6. Melanin suppression of chemokine secretion is independent of phagocytosis of**
538 **melanin or *de novo* transcription, but exerts a post-translational blockade on CXCL8**
539 **secretion. (a)** H292 cells were incubated with DMSO vehicle control or cytochalasin D (CytoD;
540 20μM) for 30 min, then stimulated with TNFα (100 ng/mL) and/or *Aspergillus* melanin ghosts (MG;
541 $2x10^7/cm^2$) for 6h. Apical CXCL8 levels were measured by ELISA. n=3. **(b)** H292 epithelium was
542 exposed to Actinomycin D (1μg/mL), then stimulated as described in A. CXCL8 apical secretion
543 was measured using an ELISA assay. One-Way ANOVA with Tukey's multiple comparisons test;
544 **p<0.01; ****p<0.0001. n=3. **(c-d)** CXCL8 expression in H292 cells lysates was measured by **(c)**
545 qPCR for RNA and **(d)** Western blot for intracellular protein, respectively, following 6h stimulation
546 with *A. fumigatus* wildtype (WT; B5233 strain; $1x10^7/cm^2$), *ΔpksP* conidia ($1x10^7/cm^2$) ± MG, *P.*
547 *aeruginosa* PAO1 strain (PSA) ± MG, or MG alone ($5x10^7/cm^2$). For Western blots, GAPDH was
548 used as a loading control. See also Figure S5. n=2. Data are represented as mean ± SEM.
549
550 **Figure 7. Epithelial calcium fluxing dampened by fungal melanin. (a)** H292 cells were
551 stimulated with media (HBSS) alone or melanin ghosts for 30 min followed by a 1 h incubation
552 with ionomycin (2 μM) and calcium chloride (1.3 mM) for 2h. Calcium fluxing measured by plate

553 reader every 15 sec. Cell stimulated with media in the presence or absence of melanin ghosts
554 produced virtually identical values. **(b)** Representative DIC (top panel) and confocal (bottom
555 panel) images of H292 calcium fluxing by fluo-4 in the presence or absence of melanin ghosts
556 when treated with media alone (HBSS without calcium or magnesium) or ionomycin and calcium.
557 Images from 10 min timepoint. Scale bar = 10 μm.
558
559 **Figure 8. Melanin disrupts actin structure in airway epithelial cells. (a)** Representative
560 images of phalloidin (green) and DAPI (blue) stained H292 cells stimulated with media alone
561 (HBSS), *P. aeruginosa* PAO1 strain (PSA; $1x10^7/cm^2$) ± MG, or MG alone ($5x10^7/cm^2$) for 6h.
562 Scale bar = 10 μm. **(b)** Representative of F actin (top blot), G actin (1:20 dilution; middle blot),
563 and total actin (bottom blot) measured by Western blot from three independent experiments. H292
564 cells were stimulated with medial alone (HBSS), *P. aeruginosa* PAO1 strain (PSA; $1x10^7/cm^2$) ±
565 MG, or MG alone ($5x10^7/cm^2$), DMSO vehicle control, or latrunculin A (LatA) for 6h. Phalloidin
566 was additionally used as a positive control. **(c)** Quantification of F/G actin ration from (b).
567

568 # Materials and Methods

569 ### *H292 culture, upright and inverted Transwell culture*

570 Human NCI-H292 pulmonary mucoepidermoid carcinoma cell line (H292) (American Type Cell
571 Collection) was grown as previously described[28,47,66,67]. H292 cells were cultured in complete
572 RPMI medium (cRMPI) (RPMI 1640, L-glutamine, 10% heat-inactivated fetal bovine serum [FBS]
573 (Gibco) and 1% penicillin/streptomycin) at 37°C in the presence of 5% CO_2. For upright Transwell
574 culture, the apical compartments of Costar 6.5 mm or 12mm Transwell® inserts with 0.4 µm pore
575 polyester membrane (Corning) were treated with a 60% Ethanol, 1:1000 rat tail collagen I
576 (Corning) mixture and left open in tissue culture hood for at least 4h to allow for evaporation. H292
577 cells were then liberated with 0.25% Trypsin-EDTA (Thermo Fisher Scientific) and resuspended
578 in cRPMI. The cell suspension was seeded onto the apical surface of the Transwells and cRPMI
579 was added to the basolateral compartment. For inverted Transwell culture for use in neutrophil
580 migration assays, Costar 6.5 mm Transwell® inserts with 3.0 µm pore polyester membranes
581 (Corning) were inverted and treated with collagen. H292 cells in suspension were applied to the
582 surface of the inverted Transwells to form a small tension bubble and incubated overnight. The
583 following day, Transwells were placed upright in a Costar culture plate (Corning) and both the
584 apical and basolateral compartments were filled with cRPMI. All transwell cultures were incubated
585 at 37°C in the presence of 5% CO_2 and used on day 7.

586

587 ### *Primary human airway epithelial basal cell proliferation and upright and inverted*
588 ### *ALI Transwell culture*

589 Primary hAEC were grown as previously described[28,40,76-78]. Basal cells were cultured in small-
590 airway epithelial cell medium (SAGM) (PromoCell) supplemented with 5 µM Y-27632 (Tocris),
591 1 µM A-83-01 (Tocris), 0.2 µM DMH-1(Selleck Chemicals), and 0.5 µM CHIR99021 (Tocris) and

592 1% penicillin/streptomycin on laminin-enriched 804G-conditioned media coated plates. For
593 differentiation of basal cells into a fully pseudostratified epithelium at ALI, the apical compartments
594 of Costar 6.5 mm or 12mm Transwell® inserts with 0.4 µm pore polyester membrane (Corning)
595 were coated with 804G-conditioned media for at least 4 hours. Upon removal, a basal cell
596 suspension in SAGM was applied to the apical compartment, and SAGM was added to the
597 basolateral compartment and the transwells were incubated overnight. The following day, the
598 SAGM was replaced with PneumaCult-ALI medium (StemCell) combined 1:1 with DMEM/F-12
599 (Gibco) and incubated overnight. The media in the apical compartment was then removed to
600 establish ALI. ALI hAEC were incubated for 16-21 days wherein the apical compartment is kept
601 dry and the ALI media in the basolateral compartment is refreshed frequently.

602 For inverted ALI culture for use in neutrophil migration assays, Costar 6.5 mm Transwell®
603 inserts with 3.0 µm pore polyester membranes (Corning) were inverted and treated with 804G-
604 conditioned media. Basal cells in suspension in SAGM were applied to the surface of the inverted
605 Transwells to form a small tension bubble and incubated overnight. The following day, Transwells
606 were placed upright in a Costar culture plate (Corning) and both the apical and basolateral
607 compartments were filled with SAGM. The following day, SAGM was replaced with PneumaCult-
608 ALI medium combined 1:1 with DMEM/F-12 and incubated overnight. The media in the apical
609 compartment was then removed to establish air-liquid interface. The inverted ALI were incubated
610 for 16-21 days wherein the apical compartment is kept dry and the media in the basolateral
611 compartment is refreshed frequently. All ALI cultures were incubated at 37°C in the presence of
612 5% CO_2. Prior to use, the transepithelial electrical resistance (TEER) was measured on the day
613 of experiment to ensure that all epithelium were intact.
614

615 ***Fungal and bacterial culture***

616 *Aspergillus fumigatus* strains *Af293, CEA10, B5233, ΔpksP,* and *ΔpksP* + pksP were used. The
617 *B5233, ΔpksP,* and complemented *ΔpksP* + pksP strains were gifted by K.J. Kwon-Chung
618 (National Institutes of Health; NIH). The *Af293* and *CEA10* strains were gifted by R.A. Cramer,
619 Darmouth College. All *A. fumigatus* strains were grown at 37°C for 3 – 5 days on glucose minimal
620 media slants (GMM). Conidia were harvested by applying a sterile solution of deionized water
621 (Milli-Q, Millipore Sigma, Burlington, MA) containing 0.01% Tween 20 to each slant followed by
622 gentle surface agitation to liberate conidia using a sterile cotton-tipped swab. The solution was
623 passed through a 40 μm cell strainer to separate conidia from hyphal fragments. Conidia were
624 then washed three times with sterile PBS and counted on a LUNA™ automated cell counter
625 (Logos Biosystems). Conidia were used either on the day of harvest or stored at 4˚C overnight for
626 use the following day. For *in vitro* experiments, conidia were applied to the apical surface. For
627 animal experiments, conidia were used on the day of harvest.
628 *P. aeruginosa* strain PAO1 (ATCC) was grown overnight in 4 mL of LB liquid media at
629 37°C with shaking. Cultures were inoculated from frozen stocks of PAO1 stored at -80°C. After
630 shaking overnight, 1 mL of overnight culture was centrifuged at 16,000 g x 5 minutes and washed
631 three times in HBSS. After the final wash the *P. aeruginosa* was resuspended in 600 μl of HBSS.
632 For *in vitro* stimulations, the *P. aeruginosa* was used at a 1:100 dilution. For quantification of
633 bacterial number for *in vivo* experiments, the OD600 of a 1:10 dilution of bacteria in HBSS was
634 obtained and bacteria were diluted appropriately. For *in vitro* experiments, *P. aeruginosa* was
635 applied to the apical surface.
636

637 ***Neutrophil isolation***

638 Neutrophils were isolated from healthy volunteer donors in accordance with Massachusetts
639 General Hospital IRB-approved protocol (2015P000818) as previously described[28,67]. Briefly, 50
640 mL of blood was drawn via venipuncture into a syringe containing acid citrate-dextrose. The blood

641 was split between three 50 mL conical tubes and layered on top of a Ficoll-Paque solution, then
642 centrifuged at 1,500 *g* for 20 minutes at room temperature to obtain a buffy coat layer. Plasma
643 and mononuclear cells were removed by aspiration. Red blood cells (RBC) were removed using
644 2% gelatin sedimentation technique followed by a wash with RBC lysis buffer. The remaining
645 neutrophils were washed and resuspended in HBSS without calcium or magnesium (HBSS-) to a
646 concentration of 5 x 10^7 neutrophils/mL.
647

648 ***Neutrophil transmigration experiments***

649 The neutrophil transepithelial migration experiments were performed as previously described
650 (**Figure 1a**)[28,40,41,67]. H292 cell monolayers or primary hAEC were grown on the underside of 3.0
651 μm pore size Transwell filters (Corning Life Sciences) to enable neutrophil migration through the
652 Transwell. Mature epithelium (at least 16 days at ALI for primary hAECs or day 7 monolayers of
653 H292 cells) in 12 well format were used for all experiments. On the day of the experiment,
654 Transwells were equilibrated in HBSS for at least 30 minutes prior to stimulation. Transwells were
655 then inverted into a sterile 15 cm cell culture plate and infected on the apical surface. Cells were
656 stimulated with media only (HBSS), *P. aeruginosa* (PAO1), *A. fumigatus* conidia, melanin ghosts,
657 or melanin ghost plus 3,000 pg/mL exogenous CXCL8 (#208-IL; R&D Systems). Infections were
658 for 1 h on H292 cell monolayers and for 2 h on primary hAEC. After stimulation, the apical surface
659 was washed and transwells were inverted into fresh 24 well culture plates containing HBSS alone
660 or HBSS containing 100 nM *N*-formyl-methionyl-leucyl-phenylalanine (fMLP; Sigma; uninfected
661 positive control). Neutrophils were applied to the basolateral compartment and transmigration was
662 allowed to proceed for 2h (H292 cells) and 4h (primary hAECs) at 37°C with 5% CO_2. After the
663 migration period, the Transwells were discarded and the migrated neutrophils were quantified
664 using a myeloperoxidase (MPO) assay. The migrated neutrophils in the apical compartment were
665 lysed with 0.5% Triton X-100 and neutrophil MPO activity was quantified using a colorimetric

666 assay using citrate buffered 2,2'-azino-bis(3-ethylbenxothiazoline-6-sulfonic acid) diammonium
667 salt (ABTS) solution (Sigma-Aldrich). After 10 min of incubation, the optical density at 405 nm was
668 read using a spectrophotometer plate reader. In addition, to the experimental samples, a standard
669 curve was prepared for each experiment was used to determine the number of migrated
670 neutrophils based on the OD_{405} value. Data are displayed as the number of transmigrated
671 neutrophils, extrapolated from the standard curve.
672

673 ***Melanin ghost preparation***

674 Melanin ghosts were prepared using previously published methods[20,34-38]. In addition to melanin
675 ghosts created in our lab using the following protocol, we also tested melanin ghosts created in
676 the laboratory of Dr. George Chamilos with similar results to our own. Briefly, *A. fumigatus* strain
677 B5233 was grown for 3 days in T75 flasks (CELLTREAT) on GMM at 30°C. *C. neoformans* strain
678 H99 (gift from Arturo Casadevall) was grown in liquid L-dopa media and incubatefd at 30°C for
679 10-14 days. Flasks were seeded from frozen stocks maintained at −80°C. To harvest fungal
680 organisms, a sterile solution of deionized water (Milli-Q; Millipore Sigma) containing 0.01% Tween
681 20 (Sigma-Aldrich) was added to each flask, and spores were liberated using gentle surface
682 agitation with a sterile swab. The spore solution was passed through a 40-µm cell strainer to
683 separate hyphal debris. To remove the fungal cell wall, *s*pores were washed three times with
684 sterile PBS, then resuspended in 10mg/mL lysing enzymes from *Trichoderma harzianum* which
685 has since been discontinued and replaced with 5mg/mL lyticase from *Arthrobacter luteus* (Sigma-
686 Aldrich) dissolved in a 1 M Sorbitol (Sigma-Aldrich) / 0.1 M Sodium Citrate (Sigma-Aldrich)
687 solution in deionized water. The solution was incubated in a 30°C water bath for 24h. To denature
688 proteins, the spore solution was then washed twice with sterile PBS and resuspended in a 4 M
689 guanidine thiocyanate (Sigma-Aldrich) solution and incubated at room temperature for 18h with
690 nutation. To hydrolyze proteins, spores were then washed twice with sterile PBS and
691 resuspended in a 1.0 mg/mL Proteinase K (Roche Laboratories) in 10mM Tris-HCl (Sigma-

692 Aldrich), 1mM $CaCl_2$ (Sigma-Aldrich), and 0.5% Sodium Dodecyl Sulfate (Sigma-Aldrich) pH 7.8,
693 solution in distilled water. The suspension was incubated in a 65°C water bath for 4h, then washed
694 three times with sterile PBS and resuspended in a 0.9% NaCl solution. A Folch lipid extraction
695 was then performed wherein the suspension was transferred to a separatory funnel along with
696 methanol (Thermo Fisher Scientific) and chloroform (Midland Scientific) and mixed vigorously.
697 This was repeated twice, with the organic layer being drained each time and the soluble melanin-
698 containing interfacial layer maintained. For the hydrolysis of residual acid-labile constituents, 6M
699 HCl (Thermo Fisher Scientific) was added to the flask and boiled for 1 hour, then combined with
700 equal volume sterile PBS to neutralize pH. The melanin ghost suspension was then washed with
701 sterile PBS and placed in 0.22 µm centrifugal filter units (Merck Millipore Ltd). The melanin ghosts
702 were then washed 3 times and resuspended in deionized water. The suspension was frozen
703 overnight at -80°C and lyophilized for two days. The melanin ghosts were finally resuspended in
704 sterile PBS, sonicated, and counted on a LUNA automated cell counter (Logos Biosystems).
705

706 ***Fungal-like particle (FLP) creation***

707 We have previously created FLP using purified fungal carbohydrates which we can associated
708 with amine-coated polystyrene 3 µM microspheres (Polysciences) using either chemical
709 conjugation or adsorption[57,58]. To create melanin-coated particles, synthetic melanin (Sigma) was
710 sonicated robustly in DMSO to create a fine suspension that was then incubated with amine-
711 coated polystyrene microspheres for 1h at room temperature with shaking. The microspheres
712 were washed copiously with PBS to remove all traces of DMSO and free melanin particles. All of
713 the microspheres obtained a brown coloration consistent with melanin association and there was
714 no free melanin visible in the flow through from the FLP.

715

716 ***ELISA***

717 Mature epithelium (at least 16 days at ALI for primary hAECs or day 7 monolayers of H292 cells)
718 in either 12 or 24 well format were used for all experiments. On the day of the experiment, growth
719 media was removed and cells were equilibrated for at least 30 min in HBSS. HBSS was removed
720 and replaced with fresh HBSS alone or containing the appropriate stimulants. Since the primary
721 hAEC are pseudostratified epithelium, the concentration of applied stimuli was based upon the
722 surface area of the epithelium rather than an MOI calculation. After application of stimuli, cell
723 culture plates were spun gently at 250 *g* x 5 min to bring pathogens in contact with epithelial
724 surface. Stimulations were allowed to proceed for the desired time (4h – 24h). Supernatants were
725 harvest and centrifuged through Captiva 96 well 0.2 uM filter plate (Agilent Technologies) at 625
726 *g* for 10 min. Supernatants were frozen at -80°C until use. Unless otherwise noted, supernatants
727 measured were from the apical side. ELISAs were performed using either R&D Duoset kits (R&D
728 Systems) or Biolegend LegendPlex assays (Legendplex™ Custom Panel (Human CXCL8, IL-8))
729 according to the manufacturers instructions. For the R&D Duoset kits the ELISA were read using
730 an i3X Spectrophotometer (Molecular Devices, LLC). For the LegendPlex assays, a BD
731 FACSCelesta™ Flow Cytometer (BD) was used for data acquisition. The resultant flow cytometry
732 files were then analyzed using the LEGENDplex™ Data Analysis Software Suite. Results were
733 analyzed using GraphPad PRISM9 software (GraphPad Software). All reported ELISAs were
734 done in both technical and biological triplicate.

735 For cytochalasin D experiments, cytochalasin D (Sigma-Aldrich) was added to HBSS
736 media at a final concentration of 20 μM. Epithelial cells were incubated for 30 min at 37°C prior to
737 stimulation. At that time the media was exchanged for fresh HBSS containing the indicated
738 stimulants in addition to 20 μM cytochalasin D. To inhibit transcription, actinomycin D (Sigma-
739 Aldrich) dissolved in DMSO was added to HBSS at a final concentration of 1μg/mL. An equal
740 volume of DMSO in HBSS was added to the control wells. Epithelial cells were then incubated for
741 1h at 37°C prior to stimulation.

742

743 **In vivo *neutrophil recruitment experiment***

744 C57BL/6 mice of 6 -12 weeks of age were obtained from Jackson Laboratories and housed in the
745 Massachusetts General Hospital specific pathogen-free animal facilities for at least one week
746 prior to infection. *Pseudomonas* strain PAO1 was diluted and quantified using OD600. Inoculums
747 were prepared consisting of HBSS alone, 5.8 x 10^5 CFU PAO1 alone, 5.8 x 10^6 melanin ghosts
748 alone, or a 5.8 x 10^5 CFU PAO1 combined with 5.8 x 10^6 melanin ghosts. Each inoculum was
749 prepared in 50 μl total volume in HBSS. Mice were infected via oropharyngeal aspiration of the
750 inoculum under isoflurane anesthesia. Infection was allowed to proceed for 4 hours, at which time
751 mice were euthanized using CO_2. Mice were exsanguinated, and the trachea was exposed and
752 cannulated with a 22G catheter (Exel Safelet Catheter) that was secured in place using suture
753 string. The lungs were flushed with a total of 2.3 ml of PBS containing 5% fetal bovine serum. The
754 collected bronchoalveolar lavage fluid was centrifuged at 300 g x 5 min to pellet cells. The pelleted
755 cells were resuspended in FACS buffer (PBS + 1% bovine serum albumin + 2 mM EDTA + 0.1%
756 sodium azide) containing 1:100 dilution of Fc Block and a 1:250 dilution of Zombie Violet dye
757 (423113; Biolegend). After incubation at 4°C for 15 minutes, cells were centrifuged and then
758 resuspended in FACS buffer containing an antibody cocktail consistent of anti-CD11b AF488
759 (101217; Biolegend), anti-CD45 APC/Cy7 (157618; Biolegend), anti-F4/80 AF647 (123122;
760 Biolegend), anti-SiglecF PE (155506; Biolegend), and anti-Gr-1 BV650 (108442; Biolegend).
761 After incubation at 4°C for 20 min cells were washed with FACS buffer and then fixed in 2%
762 paraformaldehyde for 10 min at room temperature. Cells were washed and then resuspended in
763 FACs buffer and stored at 4°C (cells were stored no longer than overnight prior to flow cytometry).
764 Splenocytes for a single mouse were prepared in parallel to use as controls for flow cytometry
765 gating. Counting beads were added prior to flow and calibration beads were prepared using each
766 of the fluorophores. Samples were run on a a BD FACSCelesta™ Flow Cytometer, neutrophils

767 were identified as $CD45^+F4/80^-SiglecF^-CD11b^+Gr\text{-}1^+$ cells, and analysis was performed using
768 FlowJo 10 software (BD). Five to six mice were used per experimental group. All animal studies
769 were conducted under protocols approved by the Institutional Animal Care and Use Committee
770 Subcommittee on Research Animal Care at Massachusetts General Hospital.
771

772 ***RNA extraction and qRT-PCR***

773 Epithelium was grown on 0.4 μm pore-size Transwells until mature (at least 16 days hAEC or 7
774 days for H292 cells). On the day of stimulation, media was removed and cells were equilibrated
775 in HBSS for at least 30 min prior to stimulation with either media alone (HBSS), *Pseudomonas*
776 *aeruginosa* (PAO1), *A. fumigatus* conidia or melanin ghosts alone or in combination. Conidia were
777 applied at 1×10^7 conidia per cm^2 and melanin ghosts were applied at 5X concentration at 5×10^7
778 conidia per cm^2. After 6h of stimulation, supernatants were harvested for ELISA. At least 4
779 Transwells of epithelium were stimulated per condition, one well of epithelium was used for
780 Western blot analysis and three wells were each harvested for RNA. For RNA prep, the epithelium
781 was washed with ice-cold HBSS and then RNA was isolated using the QIAGEN RNeasy Mini Kit.
782 After harvest of cell lysates in QIAGEN RLT buffer containing beta-mercaptoethanol, cell lysates
783 were transferred to QIAGEN QIAshredder columns to homogenize the cells, the rest of the RNA
784 extraction was performed according to RNeasy mini kit instructions. RNA was quantified using
785 nanodrop. cDNA was created using the SuperScript IV VILO kit (Thermo Fisher Scientific)
786 according to manufacturers instructions. qRT-PCR was performed on cDNA using the Taqman®
787 Fast Advanced Master Mix (Thermo Fisher Scientific) and Taqman® Gene Expression assay
788 probes CXCL8 labelled with FAM (#4331182;Hs00174103_m1; Thermo Fisher Scientific) and
789 GAPDH labelled with VIC-MGB(#448480;Hs99999905_m1; Thermo Fisher Scientific). qRT-PCR
790 reactions were run using the Applied Biosystems™ 7500 Fast Real-Time PCR System per kit

791 instructions and analyzed using the ΔΔCt method. All qRT-PCR experiments were performed in
792 at least biological duplicates.
793
794 ***Western blot***
795 Epithelium were prepared as described in "RNA extraction and qRT-PCR". After 6h of stimulation
796 the epithelium was placed on ice and lysed with 1% NP40 lysis buffer containing protease
797 inhibitor. Following denaturation with NuPAGE LDS Sample Buffer (Thermo Fisher Scientific)
798 proteins were resolved by SDS-PAGE on NuPAGE gels (NuPAGE gels, Thermo Fisher
799 Scientific). Proteins were then transferred to methanol-activated PDVF membrane (Perkin Elmer)
800 using transfer buffer (0.025M Tris, 0.192 M glycine, 20% methanol) and electrophoretic transfer
801 at 100V for 1h. The membranes were blocked for 1h at room temperature in 5% Milk in PBS-
802 0.01% Tween 20 (PBST), and then incubated with anti-CXCL8 antibody (#99407; Cell Signaling
803 Technologies) overnight at 4°C. The G-actin/F-actin assay biochem kit (#BK037; Cytoskeleton,
804 Inc.) was used for F/G actin fractionation experiments. Latrunculin A at a concentration of 10 μM
805 and 1:100 phalloidin were used as positive controls for G actin and F actin, respectively. Phalloidin
806 was added post lysate-collection as described in manufacture instructions for the kit. Membranes
807 were washed and incubated for 1h at room temperature with secondary HRP conjugated antibody
808 (#P0447; DAKO). After washing, membranes were visualized using Western Lightning Plus ECL
809 chemiluminescent substrate (Perkin Elmer, Waltham, MA) and developed using Kodak BioMax
810 XAR film (Millipore Sigma). Films were then scanned and processed using Adobe Photoshop
811 2021. Any contrast adjustments were applied evenly to the entire image and adheres to the
812 standards set forth by the scientific community[79]. All reported western blots were repeated in at
813 least biological duplicate.
814
815 ***Calcium flux plate assay***

816 H292 cells were seeded into a 96-well plate at a density of $2x10^4$ cells/well and incubated
817 overnight at 37°C with 5% CO_2 and 95% humidity. The cells were washed in serum-free cRPMI
818 medium and treated with 5 nM Fluo-4 calcium indicator dye (Invitrogen, Thermo Fisher Scientific,
819 Massachusetts, USA) with Pluronic (Invitrogen) for 1h at 37°C with 5% CO_2 and 95% humidity.
820 Subsequently, the cells were washed with HBSS without calcium and magnesium (14175-095;
821 Gibco) and pre-treated with *A. fumigatus* melanin ghosts or media (HBSS) alone for 30 min at
822 room temperature. Melanin ghosts were removed by washing and cells were stimulated with 2μM
823 ionomycin and 1.3 mM calcium chloride for 2h. Data was collected during the stimulation with 30
824 second intervals using a SpectraMax i3x Plate Reader (Molecular Devices, California, USA).
825

826 ***Confocal imaging***

827 For calcium flux assay, H292 cells were plated in Nunc Lab-Tek 8-chambered coverglass
828 (Thermo Fisher Scientific, Rochester, NY) and allowed to adhere. Cells were grown in HBSS
829 without calcium and magnesium. Fluo-4 in DMSO was added to cells for 1 h at 37°C in the dark.
830 Cells were washed and then stimulated with 2μM ionomycin and 1.3 mM calcium chloride in the
831 presence or absence of melanin ghosts. Cells were imaged every minute for 15 minutes (as
832 described below).

833 For phalloidin staining, H292 cells were plated in Nunc Lab-Tek 8-chambered coverglass (Thermo
834 Fisher Scientific, Rochester, NY) and allowed to adhere. Cells were stimulated with for 6 h,
835 washed with cold PBS, incubated with glyoxal solution for 1 h at room temperature, and quenched
836 with 50mM NH_4Cl at room temperature. Cells were permeabilized with Triton X-100 for 4 min at
837 room temperature. Non-specific binding in cells was prevented by incubating with blocking buffer
838 (5% gelatin from bovine skin [Sigma Aldrich]) for 15 min. Cells were incubated overnight at 4ºC
839 with phalloidin iFlur 488 conjugate antibodies (Caymen Chemical) in dilution buffer (PBS, 1%
840 BSA). Following three PBS washes, the chambered coverglass was then mounted with

841 Vectashield Antifade Mounting Medium (Vector Laboratories, Burlingame, CA) and Prolong
842 antifade with DAPI (Invitrogen).

843 Images were captured on a Nikon Ti-Eclipse inverted microscope equipped with a CSU-X1
844 confocal spinning-disk head (Yokogawa, Sugarland, TX) and Coherent 4W continuous-wave
845 laser (Coherent, Santa Clara, CA) excited the sample. A high-magnification, high-numerical
846 aperture objective (Nikon, 100x, 1.49 numerical aperture, oil immersion) was used. Images were
847 obtained using an EM-CCD camera (Hamamatsu, Bridgewater, NJ). Image acquisition was
848 performed using MetaMorph software version 7.10.5.476 (Molecular Devices, Downingtown, PA).
849 Raw images were then cropped using Adobe Photoshop CS5 and assembled in Adobe Illustrator,
850 version CS4 (Adobe Systems, San Jose, CA).

851

852 ***Luminex assay***

853 24-well Transwells were prepared using basal epithelial cells from three healthy human donors
854 and differentiated for 16 days at ALI. On the day of stimulation, ALI media was removed and
855 epithelium were equilibrated in HBSS media for 1.5 h prior to stimulation. The HBSS was removed
856 and replaced with fresh HBSS media on the basolateral side, and 200 μL of HBSS media
857 containing 1 x 10^7/cm^2 wild type conidia (strains *CEA10*, *Af293*, *B5233*), *ΔpksP* conidia or *P.*
858 *aeruginosa* strain PAO1. After 4h, the apical and basolateral media was harvested and put
859 through a Captiva 96 well 0.2 μm filter plate at 3000 rpm for 10 min. Supernatants were frozen at
860 -80°C. Data were processed using the Luminex analytical software. MILLIPLEX Map Human
861 cytokine/chemokine Magnetic Bead Panel – Premixed 41 Plex (Millipore Sigma), run on a
862 MAGPIX® xMAP instrument according to manufacturer's instructions. Analysis was performed
863 using GraphPad Prism.

864

865 **Pseudomonas *epithelial association assay***

866 H292 epithelium were infected with PAO1 alone or in combination with $5x10^7$ *Aspergillus* melanin
867 ghosts and incubated for 4h. Wells were washed three times with HBSS to remove any
868 nonadherent bacteria. To lyse epithelial cells, 1% Triton X-100 was added to each well, and plates
869 were incubated with gentle agitation for 1h at 4°C. The lysate was collected, vortexed, and 1:10
870 serial dilutions were made in HBSS. 100 μL of each dilution was plated onto LB agar plates
871 containing ampicillin and spread using glass beads. The plates were incubated at 37°C overnight
872 and colony forming units were counted the following day.

873

874 ***LDH viability assay***

875 The LDH viability assay was performed using Invitrogen CyQUANT LDH Cytotoxicity Assay
876 (Fisher Scientific) according to the manufacturers instructions. After 6h infection of H292 cells, a
877 1:10 dilution of 1% Triton X-100 was added to control well containing unstimulated epithelium to
878 lyse the cells and incubated for 10 min at 37°C 5% CO_2. 50 μL of supernatant from each
879 experimental condition (all experimental conditions were performed in triplicate) was transferred
880 to a 96 well plate and mixed with 50 μL of the kit Reaction mixture and allowed to incubated for
881 30 min at room temperature in the dark. Stop solution was then added to each sample and
882 absorbance at 490 and 680 was measured using an i3X Spectrophotometer (Molecular Devices,
883 LLC). LDH activity and % cytotoxicity were calculated according to assay kit instructions.

884

885 # REFERENCES

886

887 1 Thompson, G. R., 3rd & Young, J. H. *Aspergillus* infections. *N Engl J Med* **385**, 1496-
888 1509 (2021). https://doi.org:10.1056/NEJMra2027424

889 2 Huang, L. *et al.* Invasive pulmonary aspergillosis in patients with influenza infection: A
890 retrospective study and review of the literature. *Clin Respir J* **13**, 202-211 (2019).
891 https://doi.org:10.1111/crj.12995

892 3 Rawson, T. M. *et al.* Bacterial and fungal coinfection in individuals with coronavirus: a
893 rapid review to support COVID-19 antimicrobial prescribing. *Clin Infect Dis* **71**, 2459-
894 2468 (2020). https://doi.org:10.1093/cid/ciaa530

895 4 Rayens, E., Norris, K. A. & Cordero, J. F. Mortality trends in risk conditions and invasive
896 mycotic disease in the United States, 1999-2018. *Clin Infect Dis* **74**, 309-318 (2021).
897 https://doi.org:10.1093/cid/ciab336

898 5 Takazono, T. & Sheppard, D. C. *Aspergillus* in chronic lung disease: modeling what
899 goes on in the airways. *Med Mycol* **55**, 39-47 (2017).
900 https://doi.org:10.1093/mmy/myw117

901 6 Bueid, A. *et al.* Azole antifungal resistance in *Aspergillus fumigatus*: 2008 and 2009. *J*
902 *Antimicrob Chemother* **65**, 2116-2118 (2010). https://doi.org:10.1093/jac/dkq279

903 7 Iversen, M. *et al. Aspergillus* infection in lung transplant patients: incidence and
904 prognosis. *Eur J Clin Microbiol Infect Dis* **26**, 879-886 (2007).
905 https://doi.org:10.1007/s10096-007-0376-3

906 8 Lin, S. J., Schranz, J. & Teutsch, S. M. Aspergillosis case-fatality rate: systematic review
907 of the literature. *Clin Infect Dis* **32**, 358-366 (2001). https://doi.org:10.1086/318483

908 9 Ward, R. A. & Vyas, J. M. The first line of defense: effector pathways of anti-fungal
909 innate immunity. *Curr Opin Microbiol* **58**, 160-165 (2020).
910 https://doi.org:10.1016/j.mib.2020.10.003

911 10 Latgé, J. P., Beauvais, A. & Chamilos, G. The Cell Wall of the Human Fungal Pathogen
912 A*spergillus fumigatus*: Biosynthesis, Organization, Immune Response, and Virulence.
913 *Annu Rev Microbiol* **71**, 99-116 (2017). https://doi.org:10.1146/annurev-micro-030117-
914 020406

915 11 Cho, S.-H., Seo, S.-C., Schmechel, D., Grinshpun, S. A. & Reponen, T. Aerodynamic
916 characteristics and respiratory deposition of fungal fragments. *Atmospheric Environment*
917 **39**, 5454-5465 (2005). https://doi.org:https://doi.org/10.1016/j.atmosenv.2005.05.042

918 12 Valsecchi, I. *et al.* The puzzling construction of the conidial outer layer of *Aspergillus*
919 *fumigatus*. *Cell Microbiol* **21**, e12994 (2019). https://doi.org:10.1111/cmi.12994

920 13 Wang, Y., Aisen, P. & Casadevall, A. *Cryptococcus neoformans* melanin and virulence:
921 mechanism of action. *Infect Immun* **63**, 3131-3136 (1995).
922 https://doi.org:10.1128/iai.63.8.3131-3136.1995

923 14 Jahn, B. *et al.* Isolation and characterization of a pigmentless-conidium mutant of
924 *Aspergillus fumigatus* with altered conidial surface and reduced virulence. *Infect Immun*
925 **65**, 5110-5117 (1997). https://doi.org:10.1128/iai.65.12.5110-5117.1997

926 15 Langfelder, K. *et al.* Identification of a polyketide synthase gene (pksP) of *Aspergillus*
927 *fumigatus* involved in conidial pigment biosynthesis and virulence. *Med Microbiol*
928 *Immunol* **187**, 79-89 (1998).

929 16 Tsai, H. F., Chang, Y. C., Washburn, R. G., Wheeler, M. H. & Kwon-Chung, K. J. The
930 developmentally regulated *alb1* gene of *Aspergillus fumigatus*: its role in modulation of
931 conidial morphology and virulence. *J Bacteriol* **180**, 3031-3038 (1998).

932 17 Sugareva, V. *et al.* Characterisation of the laccase-encoding gene abr2 of the
933 dihydroxynaphthalene-like melanin gene cluster of *Aspergillus fumigatus*. *Arch Microbiol*
934 **186**, 345-355 (2006). https://doi.org:10.1007/s00203-006-0144-2

935 18 Chai, L. Y. *et al. Aspergillus fumigatus* conidial melanin modulates host cytokine
936 response. *Immunobiology* **215**, 915-920 (2010).
937 https://doi.org:10.1016/j.imbio.2009.10.002

938 19 Graf, K. T., Liu, H., Filler, S. G. & Bruno, V. M. Depletion of extracellular chemokines by
939 *Aspergillus* melanin. *mBio* **14**, e0019423 (2023). https://doi.org:10.1128/mbio.00194-23

940 20 Akoumianaki, T. *et al. Aspergillus* cell wall melanin blocks LC3-associated phagocytosis
941 to promote pathogenicity. *Cell Host Microbe* **19**, 79-90 (2016).
942 https://doi.org:10.1016/j.chom.2015.12.002

943 21 Goncalves, S. M. *et al.* Phagosomal removal of fungal melanin reprograms macrophage
944 metabolism to promote antifungal immunity. *Nat Commun* **11**, 2282 (2020).
945 https://doi.org:10.1038/s41467-020-16120-z

946 22 Kradin, R. L. & Mark, E. J. The pathology of pulmonary disorders due to *Aspergillus spp*.
947 *Arch Pathol Lab Med* **132**, 606-614 (2008). https://doi.org:10.5858/2008-132-606-
948 TPOPDD

949 23 Latge, J. P. The pathobiology of *Aspergillus fumigatus*. *Trends Microbiol* **9**, 382-389
950 (2001). https://doi.org:10.1016/s0966-842x(01)02104-7

951 24 Lee, J. Y. *et al. Aspergillus* Tracheobronchitis and Influenza A Co-infection in a Patient
952 with AIDS and Neutropenia. *Infect Chemother* **46**, 209-215 (2014).
953 https://doi.org:10.3947/ic.2014.46.3.209

954 25 Nyga, R. *et al.* Invasive Tracheobronchial Aspergillosis in Critically Ill Patients with
955 Severe Influenza. A Clinical Trial. *Am J Respir Crit Care Med* **202**, 708-716 (2020).
956 https://doi.org:10.1164/rccm.201910-1931OC

957 26 Montoro, D. T. *et al.* A revised airway epithelial hierarchy includes CFTR-expressing
958 ionocytes. *Nature* **560**, 319-324 (2018). https://doi.org:10.1038/s41586-018-0393-7

959 27 Yonker, L. M. *et al.* Neutrophil-Derived Cytosolic PLA2α Contributes to Bacterial-Induced
960 Neutrophil Transepithelial Migration. *J Immunol* **199**, 2873-2884 (2017).
961 https://doi.org:10.4049/jimmunol.1700539

962 28 Feldman, M. B. *et al. Aspergillus fumigatus* Cell Wall Promotes Apical Airway Epithelial
963 Recruitment of Human Neutrophils. *Infect Immun* **88** (2020).
964 https://doi.org:10.1128/IAI.00813-19

29 Feldman, M. B., Wood, M., Lapey, A. & Mou, H. SMAD Signaling Restricts Mucous Cell Differentiation in Human Airway Epithelium. *Am J Respir Cell Mol Biol* **61**, 322-331 (2019). https://doi.org:10.1165/rcmb.2018-0326OC

30 Yonker, L. M. *et al.* Neutrophil dysfunction in cystic fibrosis. *J Cyst Fibros* **20**, 1062-1071 (2021). https://doi.org:10.1016/j.jcf.2021.01.012

31 Stappers, M. H. T. *et al.* Recognition of DHN-melanin by a C-type lectin receptor is required for immunity to *Aspergillus*. *Nature* **555**, 382-386 (2018). https://doi.org:10.1038/nature25974

32 Lopez Robles, M. D. *et al.* Cell-surface C-type lectin-like receptor CLEC-1 dampens dendritic cell activation and downstream Th17 responses. *Blood Adv* **1**, 557-568 (2017). https://doi.org:10.1182/bloodadvances.2016002360

33 Colonna, M., Samaridis, J. & Angman, L. Molecular characterization of two novel C-type lectin-like receptors, one of which is selectively expressed in human dendritic cells. *Eur J Immunol* **30**, 697-704 (2000). https://doi.org:10.1002/1521-4141(200002)30:2<697::Aid-immu697>3.0.Co;2-m

34 Wang, Y., Aisen, P. & Casadevall, A. Melanin, melanin "ghosts," and melanin composition in *Cryptococcus neoformans*. *Infect Immun* **64**, 2420-2424 (1996). https://doi.org:10.1128/iai.64.7.2420-2424.1996

35 Rosas, A. L. *et al.* Synthesis of polymerized melanin by *Cryptococcus neoformans* in infected rodents. *Infect Immun* **68**, 2845-2853 (2000). https://doi.org:10.1128/IAI.68.5.2845-2853.2000

36 Folch, J., Lees, M. & Sloane Stanley, G. H. A simple method for the isolation and purification of total lipides from animal tissues. *J Biol Chem* **226**, 497-509 (1957).

37 Chamilos, G. *et al.* Melanin targets LC3-associated phagocytosis (LAP): A novel pathogenetic mechanism in fungal disease. *Autophagy* **12**, 888-889 (2016). https://doi.org:10.1080/15548627.2016.1157242

38 Camacho, E. *et al.* N-acetylglucosamine affects Cryptococcus neoformans cell-wall composition and melanin architecture. *Microbiology (Reading)* **163**, 1540-1556 (2017). https://doi.org:10.1099/mic.0.000552

39 Pazos, M. A. *et al. Pseudomonas aeruginosa* ExoU augments neutrophil transepithelial migration. *PLoS Pathog* **13**, e1006548 (2017). https://doi.org:10.1371/journal.ppat.1006548

40 Yonker, L. M. *et al.* Development of a Primary Human Co-Culture Model of Inflamed Airway Mucosa. *Sci Rep* **7**, 8182 (2017). https://doi.org:10.1038/s41598-017-08567-w

41 Yonker, L. M. *et al.* Neutrophil-Derived Cytosolic PLA2alpha Contributes to Bacterial-Induced Neutrophil Transepithelial Migration. *J Immunol* **199**, 2873-2884 (2017). https://doi.org:10.4049/jimmunol.1700539

1002 42 Das, S. T. *et al.* Monomeric and dimeric CXCL8 are both essential for *in vivo* neutrophil
1003 recruitment. *PLoS One* **5**, e11754 (2010). https://doi.org:10.1371/journal.pone.0011754

1004 43 Long, M. B. & Chalmers, J. D. Treating Neutrophilic Inflammation in Airways Diseases.
1005 *Arch Bronconeumol* **58**, 463-465 (2022). https://doi.org:10.1016/j.arbres.2021.11.003

1006 44 Tamang, D. L. *et al.* Hepoxilin A(3) facilitates neutrophilic breach of lipoxygenase-
1007 expressing airway epithelial barriers. *J Immunol* **189**, 4960-4969 (2012).
1008 https://doi.org:10.4049/jimmunol.1201922

1009 45 Pazos, M. A. *et al.* Distinct cellular sources of hepoxilin A3 and leukotriene B4 are used
1010 to coordinate bacterial-induced neutrophil transepithelial migration. *J Immunol* **194**,
1011 1304-1315 (2015). https://doi.org:10.4049/jimmunol.1402489

1012 46 Mrsny, R. J. *et al.* Identification of hepoxilin A3 in inflammatory events: a required role in
1013 neutrophil migration across intestinal epithelia. *Proc Natl Acad Sci U S A* **101**, 7421-
1014 7426 (2004). https://doi.org:10.1073/pnas.0400832101

1015 47 Kubala, S. A., Patil, S. U., Shreffler, W. G. & Hurley, B. P. Pathogen induced chemo-
1016 attractant hepoxilin A3 drives neutrophils, but not eosinophils across epithelial barriers.
1017 *Prostaglandins Other Lipid Mediat* **108**, 1-8 (2014).
1018 https://doi.org:10.1016/j.prostaglandins.2013.11.001

1019 48 Riley, P. A. Melanin. *Int J Biochem Cell Biol* **29**, 1235-1239 (1997).
1020 https://doi.org:10.1016/s1357-2725(97)00013-7

1021 49 White, L. P. Melanin: a naturally occurring cation exchange material. *Nature* **182**, 1427-
1022 1428 (1958). https://doi.org:10.1038/1821427a0

1023 50 Wheeler, M. H. & Bell, A. A. Melanins and their importance in pathogenic fungi. *Curr Top*
1024 *Med Mycol* **2**, 338-387 (1988). https://doi.org:10.1007/978-1-4612-3730-3_10

1025 51 Rhodes, J. C., Polacheck, I. & Kwon-Chung, K. J. Phenoloxidase activity and virulence
1026 in isogenic strains of Cryptococcus neoformans. *Infect Immun* **36**, 1175-1184 (1982).
1027 https://doi.org:10.1128/iai.36.3.1175-1184.1982

1028 52 Kwon-Chung, K. J., Tom, W. K. & Costa, J. L. Utilization of indole compounds by
1029 Cryptococcus neoformans to produce a melanin-like pigment. *J Clin Microbiol* **18**, 1419-
1030 1421 (1983). https://doi.org:10.1128/jcm.18.6.1419-1421.1983

1031 53 Salas, S. D., Bennett, J. E., Kwon-Chung, K. J., Perfect, J. R. & Williamson, P. R. Effect
1032 of the laccase gene CNLAC1, on virulence of Cryptococcus neoformans. *J Exp Med*
1033 **184**, 377-386 (1996). https://doi.org:10.1084/jem.184.2.377

1034 54 Tsai, H. F., Washburn, R. G., Chang, Y. C. & Kwon-Chung, K. J. Aspergillus fumigatus
1035 arp1 modulates conidial pigmentation and complement deposition. *Mol Microbiol* **26**,
1036 175-183 (1997). https://doi.org:10.1046/j.1365-2958.1997.5681921.x

1037 55 Eisenman, H. C. *et al.* Microstructure of cell wall-associated melanin in the human
1038 pathogenic fungus Cryptococcus neoformans. *Biochemistry* **44**, 3683-3693 (2005).
1039 https://doi.org:10.1021/bi047731m

1040 56 Eisenman, H. C. *et al. Cryptococcus neoformans* laccase catalyses melanin synthesis
1041 from both D- and L-DOPA. *Microbiology (Reading)* **153**, 3954-3962 (2007).
1042 https://doi.org:10.1099/mic.0.2007/011049-0

1043 57 Tam, J. M., Mansour, M. K., Khan, N. S., Yoder, N. C. & Vyas, J. M. Use of fungal
1044 derived polysaccharide-conjugated particles to probe Dectin-1 responses in innate
1045 immunity. *Integr Biol (Camb)* **4**, 220-227 (2012). https://doi.org:10.1039/c2ib00089j

1046 58 Reedy, J. L. *et al.* The C-Type Lectin Receptor Dectin-2 Is a Receptor for *Aspergillus*
1047 *fumigatus* Galactomannan. *mBio* **14**, e0318422 (2023).
1048 https://doi.org:10.1128/mbio.03184-22

1049 59 Chow, A. W. *et al.* Polarized secretion of interleukin (IL)-6 and IL-8 by human airway
1050 epithelia 16HBE14o- cells in response to cationic polypeptide challenge. *PLoS One* **5**,
1051 e12091 (2010). https://doi.org:10.1371/journal.pone.0012091

1052 60 Pillai, D. K. *et al.* Directional secretomes reflect polarity-specific functions in an in vitro
1053 model of human bronchial epithelium. *Am J Respir Cell Mol Biol* **50**, 292-300 (2014).
1054 https://doi.org:10.1165/rcmb.2013-0188OC

1055 61 Skronska-Wasek, W., Durlanik, S., Garnett, J. P. & Pflanz, S. Polarized cytokine release
1056 from airway epithelium differentially influences macrophage phenotype. *Mol Immunol*
1057 **132**, 142-149 (2021). https://doi.org:10.1016/j.molimm.2021.01.029

1058 62 Thywißen, A. *et al.* Conidial dihydroxynaphthalene melanin of the human pathogenic
1059 fungus *Aspergillus fumigatus* interferes with the host endocytosis pathway. *Front*
1060 *Microbiol* **2**, 96 (2011). https://doi.org:10.3389/fmicb.2011.00096

1061 63 Amin, S., Thywissen, A., Heinekamp, T., Saluz, H. P. & Brakhage, A. A. Melanin
1062 dependent survival of Apergillus fumigatus conidia in lung epithelial cells. *Int J Med*
1063 *Microbiol* **304**, 626-636 (2014). https://doi.org:10.1016/j.ijmm.2014.04.009

1064 64 van den Berg, A. *et al.* Cytoskeletal architecture differentially controls post-transcriptional
1065 processing of IL-6 and IL-8 mRNA in airway epithelial-like cells. *Exp Cell Res* **312**, 1496-
1066 1506 (2006). https://doi.org:10.1016/j.yexcr.2006.01.010

1067 65 Cambier, S., Gouwy, M. & Proost, P. The chemokines CXCL8 and CXCL12: molecular
1068 and functional properties, role in disease and efforts towards pharmacological
1069 intervention. *Cellular & Molecular Immunology* **20**, 217-251 (2023).
1070 https://doi.org:10.1038/s41423-023-00974-6

1071 66 Hurley, B. P., Siccardi, D., Mrsny, R. J. & McCormick, B. A. Polymorphonuclear cell
1072 transmigration induced by *Pseudomonas aeruginosa* requires the eicosanoid hepoxilin
1073 A3. *J Immunol* **173**, 5712-5720 (2004). https://doi.org:10.4049/jimmunol.173.9.5712

1074 67 Kusek, M. E., Pazos, M. A., Pirzai, W. & Hurley, B. P. *In vitro* coculture assay to assess
1075 pathogen induced neutrophil trans-epithelial migration. *J Vis Exp*, e50823 (2014).
1076 https://doi.org:10.3791/50823

1077 68 Crossen, A. J. *et al.* Human Airway Epithelium Responses to Invasive Fungal Infections:
1078 A Critical Partner in Innate Immunity. *J Fungi (Basel)* **9** (2022).
1079 https://doi.org:10.3390/jof9010040

1080 69 Chamilos, G. & Carvalho, A. *Aspergillus fumigatus* DHN-Melanin. *Curr Top Microbiol*
1081 *Immunol* **425**, 17-28 (2020). https://doi.org:10.1007/82_2020_205

1082 70 Kyrmizi, I. *et al.* Calcium sequestration by fungal melanin inhibits calcium-calmodulin
1083 signalling to prevent LC3-associated phagocytosis. *Nat Microbiol* **3**, 791-803 (2018).
1084 https://doi.org:10.1038/s41564-018-0167-x

1085 71 Hiramatsu, Y., Nishida, T., Nugraha, D. K., Sugihara, F. & Horiguchi, Y. Melanin
1086 Produced by Bordetella parapertussis Confers a Survival Advantage to the Bacterium
1087 during Host Infection. *mSphere* **6**, e0081921 (2021).
1088 https://doi.org:10.1128/mSphere.00819-21

1089 72 Hann, J., Bueb, J. L., Tolle, F. & Bréchard, S. Calcium signaling and regulation of
1090 neutrophil functions: Still a long way to go. *J Leukoc Biol* **107**, 285-297 (2020).
1091 https://doi.org:10.1002/jlb.3ru0719-241r

1092 73 Kong, F., You, H., Zheng, K., Tang, R. & Zheng, C. The crosstalk between pattern-
1093 recognition receptor signaling and calcium signaling. *Int J Biol Macromol* **192**, 745-756
1094 (2021). https://doi.org:10.1016/j.ijbiomac.2021.10.014

1095 74 Kuhns, D. B., Young, H. A., Gallin, E. K. & Gallin, J. I. Ca2+-dependent production and
1096 release of IL-8 in human neutrophils. *J Immunol* **161**, 4332-4339 (1998).

1097 75 Waters, V. *et al.* The effect of cyclosporin A on airway cell proinflammatory signaling and
1098 pneumonia. *Am J Respir Cell Mol Biol* **33**, 138-144 (2005).
1099 https://doi.org:10.1165/rcmb.2005-0005OC

1100 76 Levardon, H., Yonker, L. M., Hurley, B. P. & Mou, H. Expansion of Airway Basal Cells
1101 and Generation of Polarized Epithelium. *Bio Protoc* **8** (2018).
1102 https://doi.org:10.21769/BioProtoc.2877

1103 77 Mou, H. *et al.* Dual SMAD Signaling Inhibition Enables Long-Term Expansion of Diverse
1104 Epithelial Basal Cells. *Cell Stem Cell* **19**, 217-231 (2016).
1105 https://doi.org:10.1016/j.stem.2016.05.012

1106 78 Mou, H. *et al.* Airway basal stem cells generate distinct subpopulations of PNECs. *Cell*
1107 *Rep* **35**, 109011 (2021). https://doi.org:10.1016/j.celrep.2021.109011

1108 79 Rossner, M. & Yamada, K. M. What's in a picture? The temptation of image
1109 manipulation. *J Cell Biol* **166**, 11-15 (2004). https://doi.org:10.1083/jcb.200406019

1110

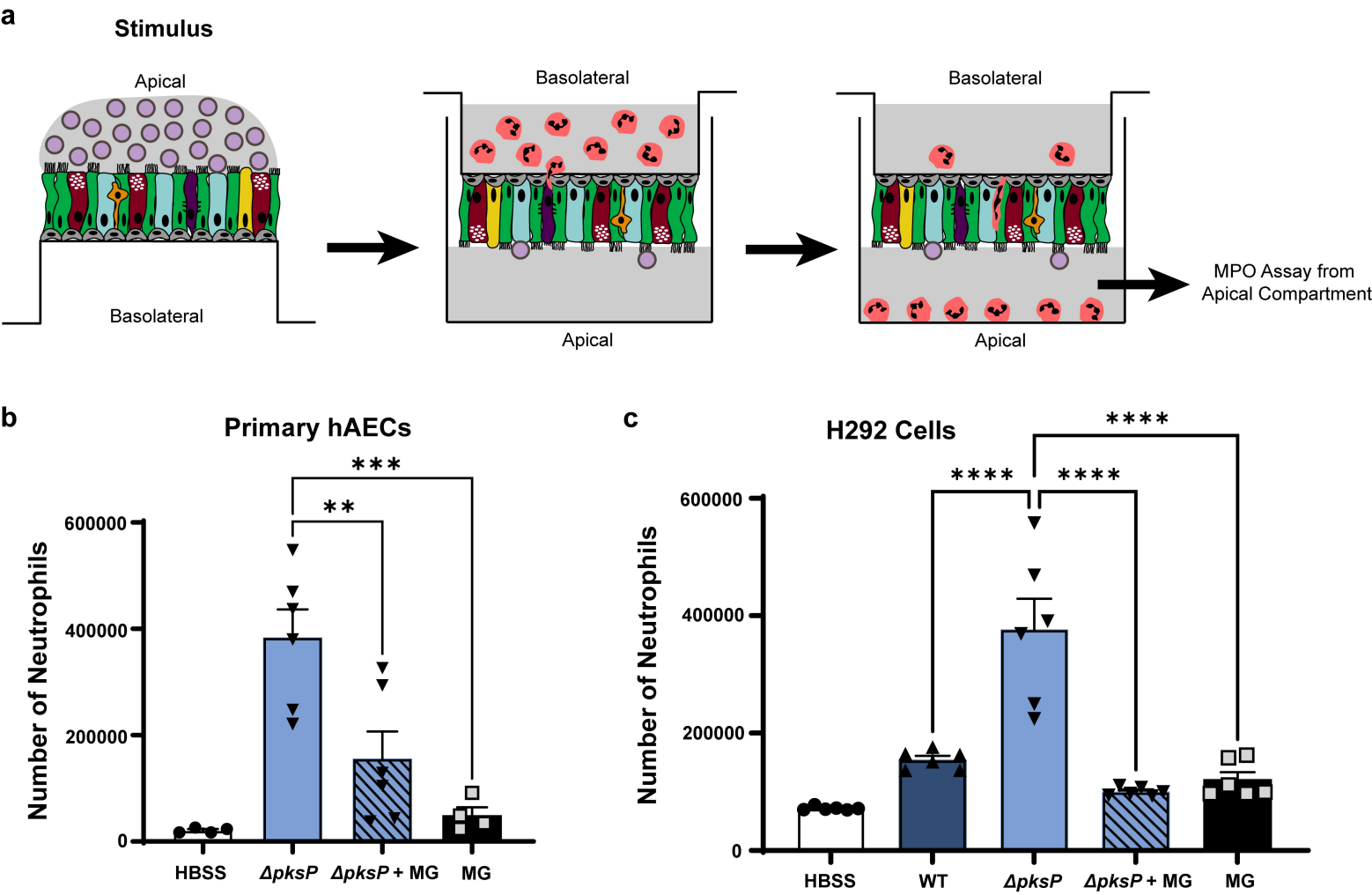
a
Stimulus
Apical
Basolateral
Basolateral
Apical
Basolateral
Apical
MPO Assay from
Apical Compartment
b
Primary hAECs
***
**
600000
400000
200000
0
Number of Neutrophils
HBSS
ΔpksP
ΔpksP + MG
MG
c
H292 Cells
****
****
****
600000
400000
200000
0
Number of Neutrophils
HBSS
WT
ΔpksP
ΔpksP + MG
MG

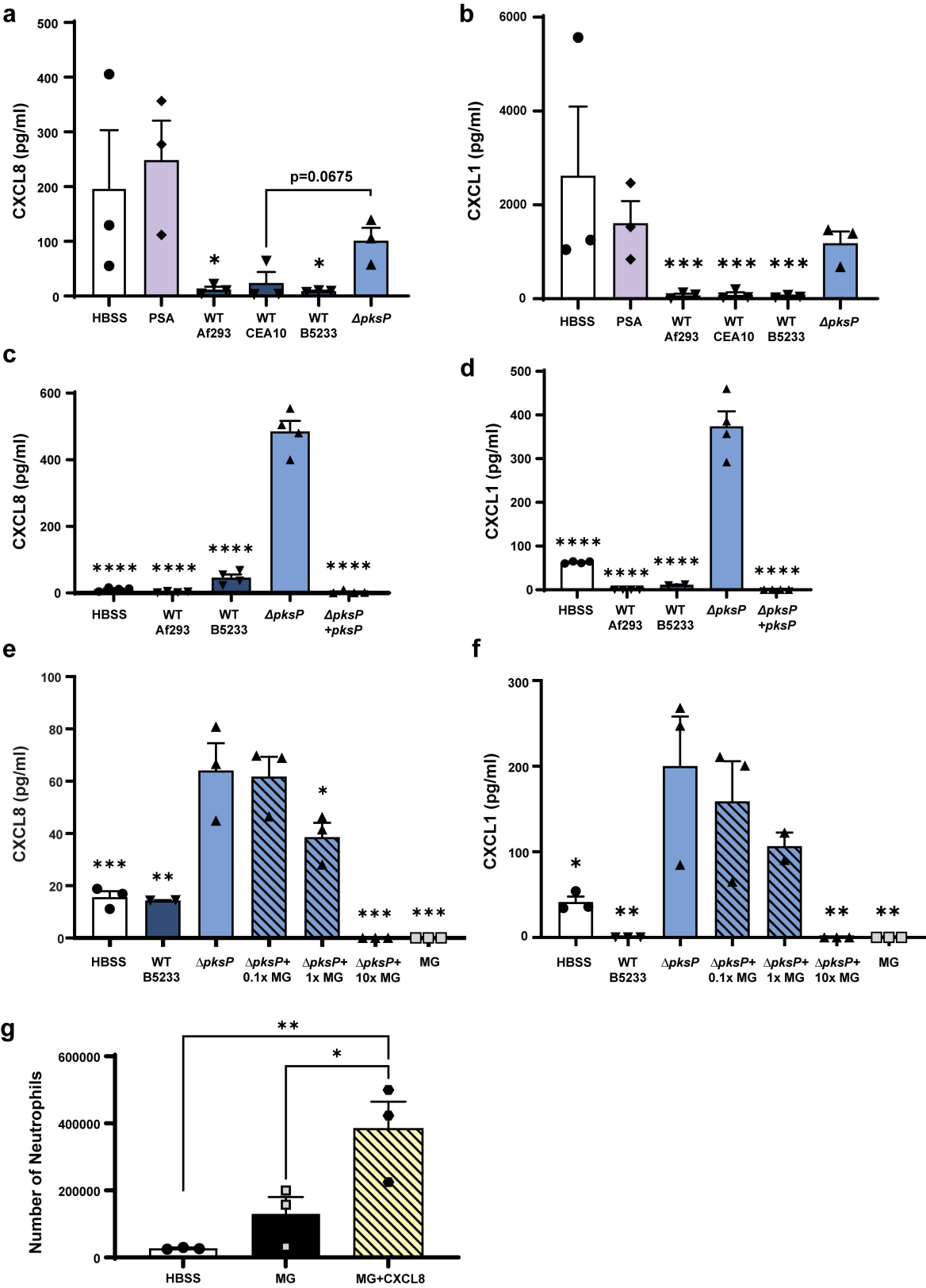
a
CXCL8 (pg/ml)
500
400
300
200
100
0
p=0.0675
*
*
HBSS
PSA
WT Af293
WT CEA10
WT B5233
ΔpksP
b
CXCL1 (pg/ml)
6000
4000
2000
0
***
***
***
HBSS
PSA
WT Af293
WT CEA10
WT B5233
ΔpksP
c
CXCL8 (pg/ml)
600
400
200
0
****
****
****
****
HBSS
WT Af293
WT B5233
ΔpksP
ΔpksP +pksP
d
CXCL1 (pg/ml)
500
400
300
200
100
0
****
****
****
****
HBSS
WT Af293
WT B5233
ΔpksP
ΔpksP +pksP
e
CXCL8 (pg/ml)
100
80
60
40
20
0
***
**
*
***
***
HBSS
WT B5233
ΔpksP
ΔpksP+ 0.1x MG
ΔpksP+ 1x MG
ΔpksP+ 10x MG
MG
f
CXCL1 (pg/ml)
300
200
100
0
*
**
**
**
HBSS
WT B5233
ΔpksP
ΔpksP+ 0.1x MG
ΔpksP+ 1x MG
ΔpksP+ 10x MG
MG
g
Number of Neutrophils
600000
400000
200000
0
**
*
HBSS
MG
MG+CXCL8

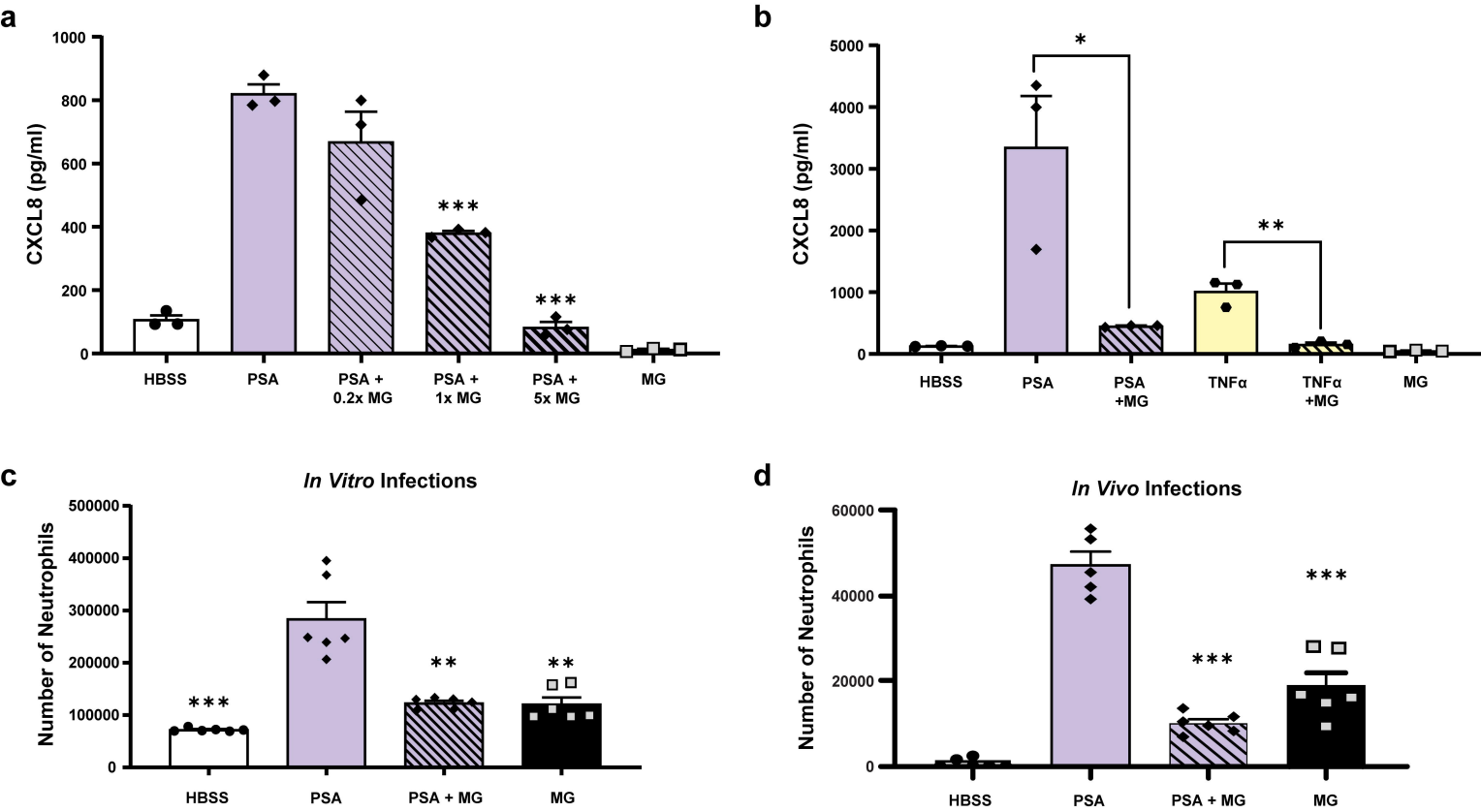
a
CXCL8 (pg/ml)
1000
800
600
400
200
0
***
***
HBSS
PSA
PSA + 0.2x MG
PSA + 1x MG
PSA + 5x MG
MG
b
CXCL8 (pg/ml)
5000
4000
3000
2000
1000
0
*
**
HBSS
PSA
PSA +MG
TNFα
TNFα +MG
MG
c
In Vitro Infections
Number of Neutrophils
500000
400000
300000
200000
100000
0
***
**
**
HBSS
PSA
PSA + MG
MG
d
In Vivo Infections
Number of Neutrophils
60000
40000
20000
0
***
***
HBSS
PSA
PSA + MG
MG

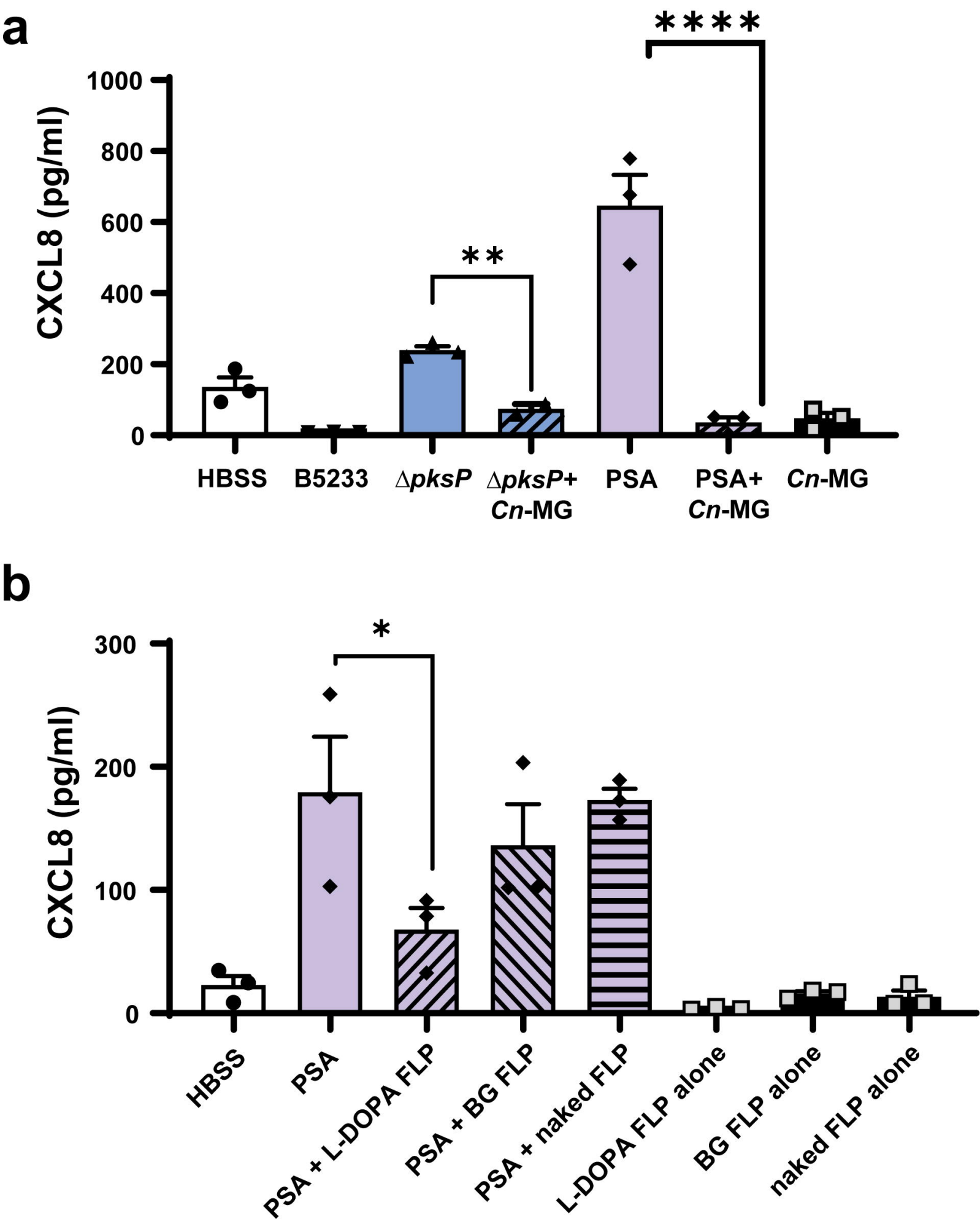
a
CXCL8 (pg/ml)
1000
800
600
400
200
0
****
**
HBSS
B5233
ΔpksP
ΔpksP+ Cn-MG
PSA
PSA+ Cn-MG
Cn-MG
b
CXCL8 (pg/ml)
300
200
100
0
*
HBSS
PSA
PSA + L-DOPA FLP
PSA + BG FLP
PSA + naked FLP
L-DOPA FLP alone
BG FLP alone
naked FLP alone

a

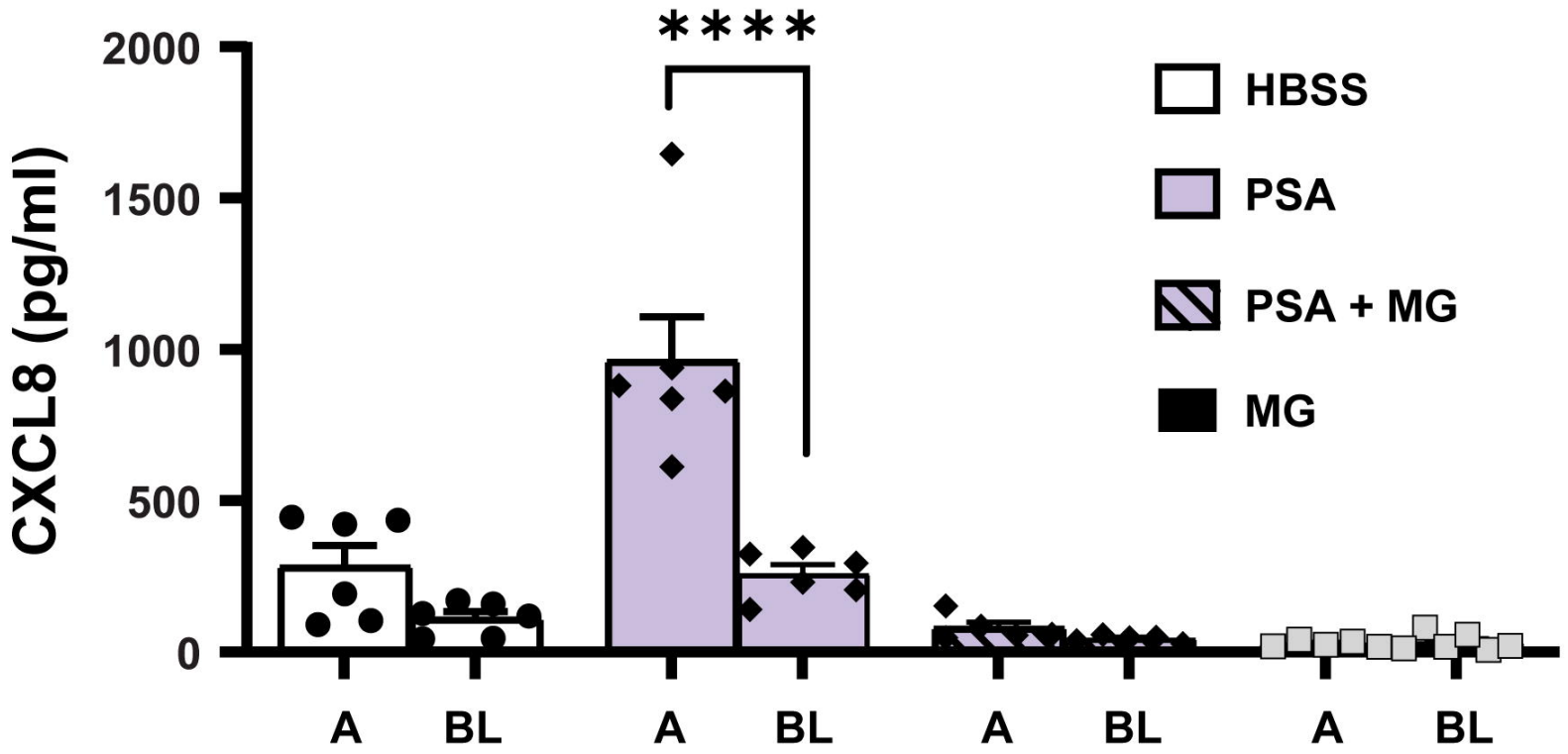
****
2000
1500
1000
500
0
CXCL8 (pg/ml)
HBSS
PSA
PSA + MG
MG
A
BL
A
BL
A
BL
A
BL

b

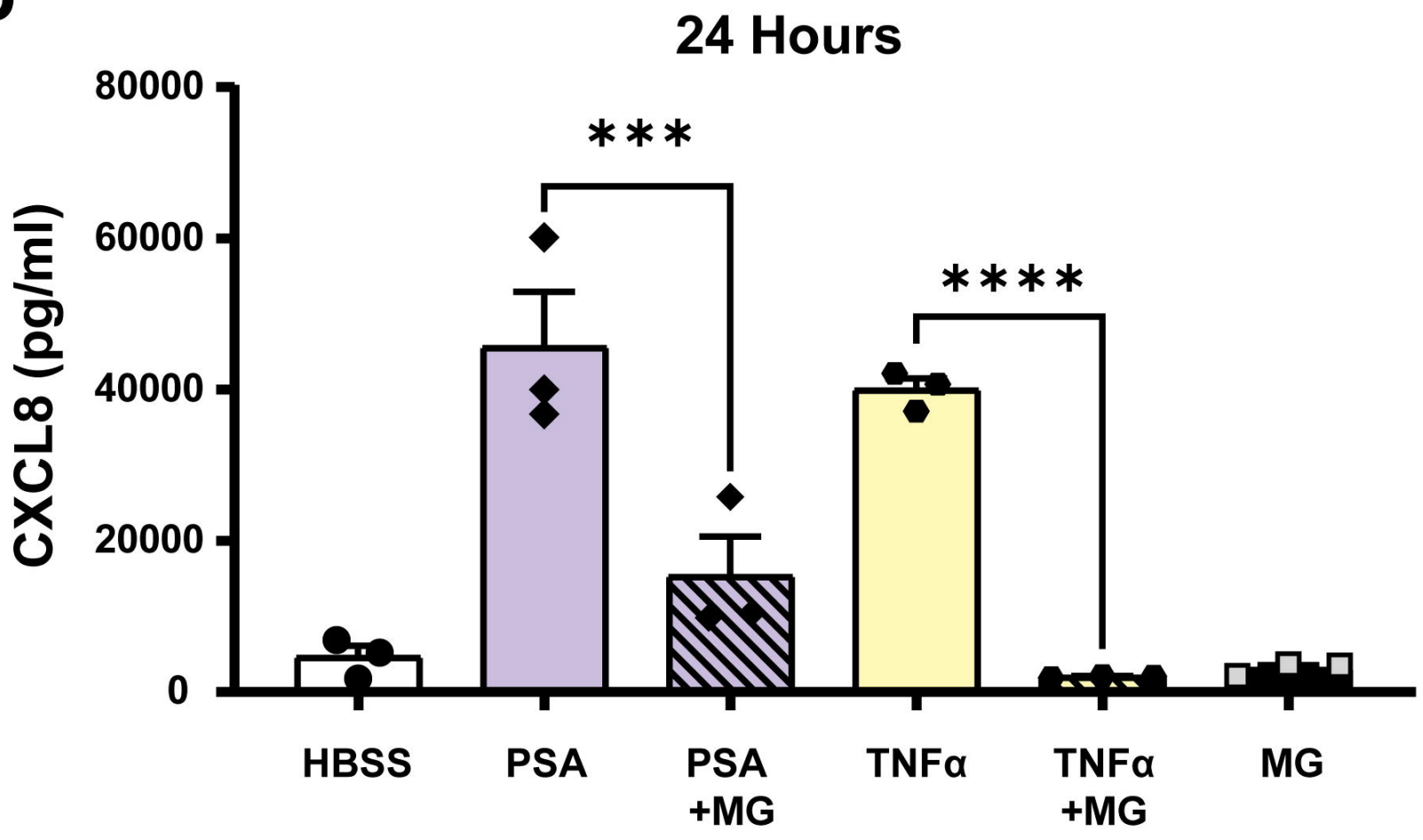
24 Hours
80000
60000
40000
20000
0
CXCL8 (pg/ml)
***
****
HBSS
PSA
PSA +MG
TNFα
TNFα +MG
MG

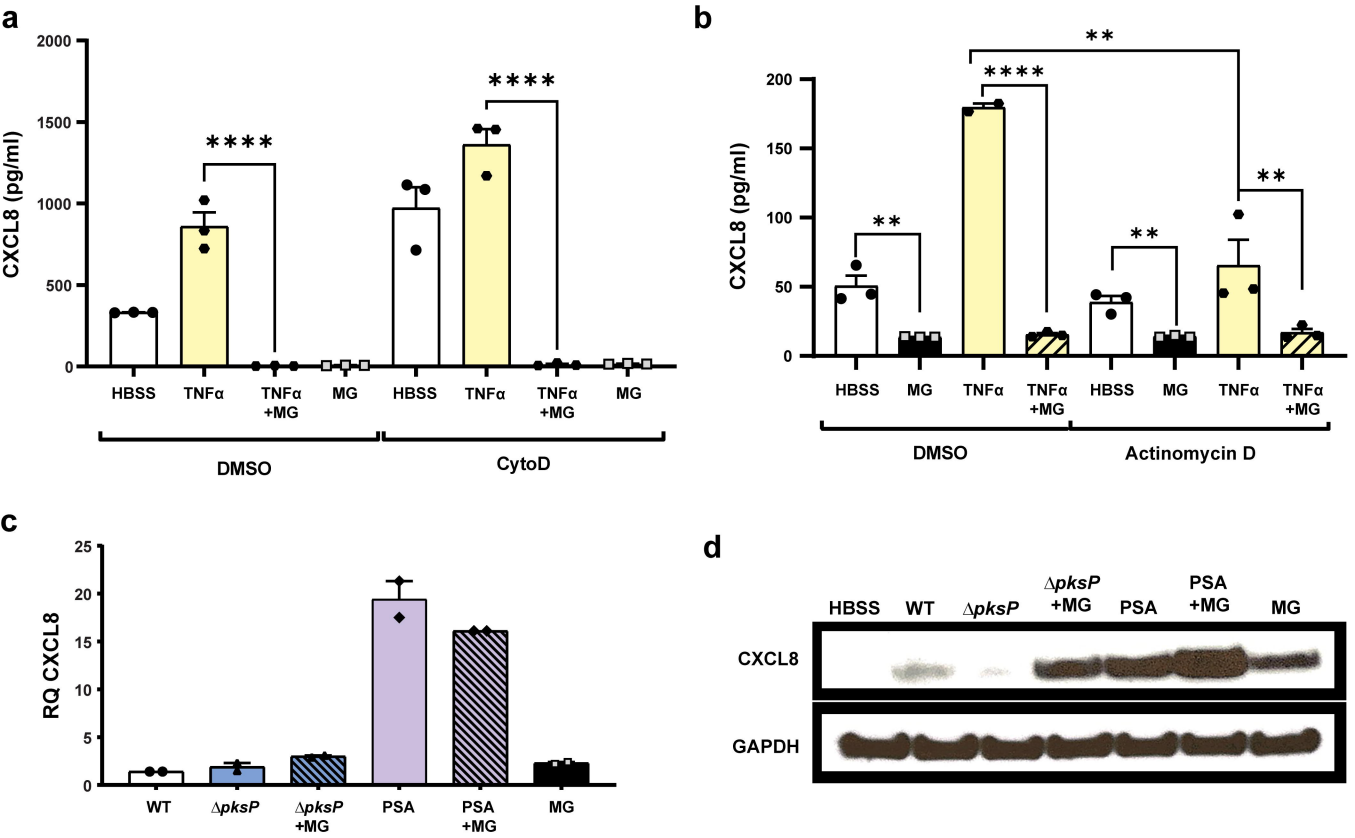
a
CXCL8 (pg/ml)
2000
1500
1000
500
0
****
****
HBSS
TNFα
TNFα +MG
MG
HBSS
TNFα
TNFα +MG
MG
DMSO
CytoD
b
CXCL8 (pg/ml)
200
150
100
50
0
**
****
**
**
**
HBSS
MG
TNFα
TNFα +MG
HBSS
MG
TNFα
TNFα +MG
DMSO
Actinomycin D
c
RQ CXCL8
25
20
15
10
5
0
WT
ΔpksP
ΔpksP +MG
PSA
PSA +MG
MG
d
HBSS
WT
ΔpksP
ΔpksP +MG
PSA
PSA +MG
MG
CXCL8
GAPDH

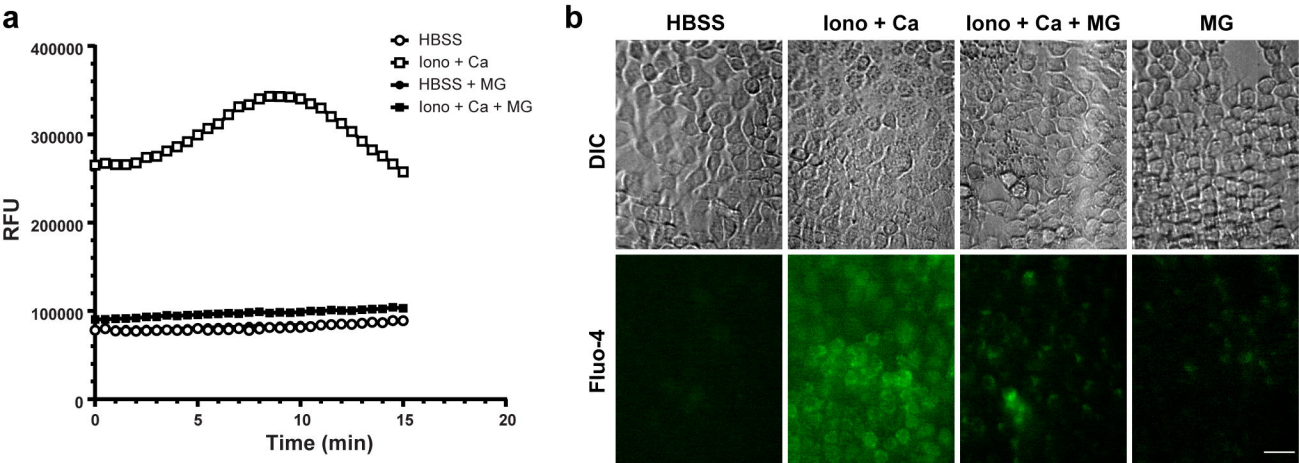
a
HBSS
Iono + Ca
HBSS + MG
Iono + Ca + MG
RFU
400000
300000
200000
100000
0
0
5
10
15
20
Time (min)
b
HBSS
Iono + Ca
Iono + Ca + MG
MG
DIC
Fluo-4

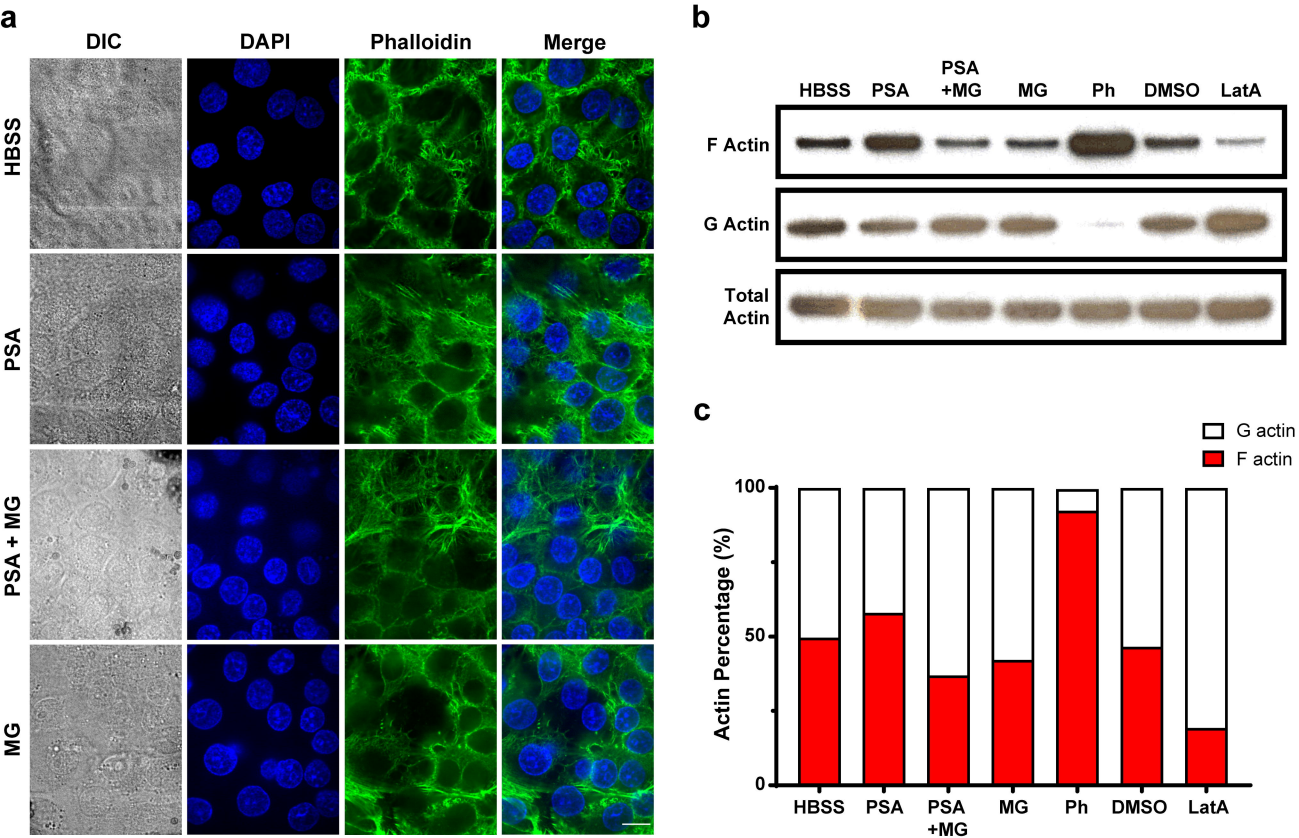
a
DIC
DAPI
Phalloidin
Merge
HBSS
PSA
PSA + MG
MG
b
HBSS
PSA
PSA +MG
MG
Ph
DMSO
LatA
F Actin
G Actin
Total Actin
c
G actin
F actin
Actin Percentage (%)
100
50
0
HBSS
PSA
PSA +MG
MG
Ph
DMSO
LatA